DESIGN SPECIFICATIONS AND REQUIREMENTS OF THE ORCHID SET-UP

Version 1.1

Adam Joseph Head, Carlo De Servi, Emiliano Casati, and P. Colonna

Delft, May 2015

Propulsion and Power Group, Delft University of Technology,
Kluyverweg 1, 2629 HS Delft, The Netherlands

Revised by	Date
Alberto Guardone	4-6-2015

Contents

Contents **2**

List of Figures **3**

List of Tables **4**

1 Introduction **5**
1.1 Background . . . 5
1.2 Motivation . . . 6
1.3 The Setup Concept . . . 7
1.4 Design Procedure . . . 8
1.5 Report Structure . . . 8

2 Thermodynamic Analysis of the BoP: Nominal Operating Conditions **9**
2.1 Cycle Configuration . . . 9
2.2 Working fluids . . . 12
2.3 Main Design Constraints . . . 13
2.4 Design of the Supersonic Nozzle Test Section . . . 14
2.5 Turbine Test Section . . . 20
2.6 Siloxane MM as the *design fluid* . . . 22
2.7 Nominal Operating Conditions . . . 23
2.8 Conclusions . . . 23

3 Requirements and Specifications for the BoP Hardware **27**
3.1 APP Laboratory Location and Layout . . . 27
3.2 Test Section Positioning . . . 30
3.3 Thermal Oil Electric Heater . . . 30
3.4 Air Coolers . . . 32
3.5 Primary Hardware . . . 33
3.6 Auxiliary Systems . . . 36

4 Requirements and Specifications for the DAQ and Control Systems **39**
4.1 Control System . . . 39
4.2 Control Loop . . . 40
4.3 Start-Up . . . 40
4.4 Measurement Instrumentation . . . 43

Bibliography **47**

List of Figures

1.1 Simplified process flow diagram of the ORCHID facility. 6
1.2 $T - s$ diagram of siloxane MM and pentane showing the state points of two possible thermodynamic Rankine cycles of interest for experiments with the ORCHID set-up. 7

2.1 Detailed process flow diagram of the ORCHID facility. 11
2.2 Exemplary thermodynamic cycles in the $T - s$ diagram of the working fluid (siloxane MM in this case). The blue lines represent the processes in common to the operation of both TS's. The red line shows the expansion process from supercritical conditions if the nozzle TS is in operation (the cycle encompasses the state points $6 - 7 - 8 - 1 - * - 3 - 4 - 5$). The asterisk highlights the thermodynamic state in the throat of the nozzle. The green line shows the expansion process if the turbine TS is in operation (the cycle encompasses the state points $6 - 7 - 8 - 1 - 4 - 5$). Numbered thermodynamic states refer to conditions at components interfaces as reported in the process flow diagram of Fig. 2.1. 12
2.3 $T - s$ Diagram of MDM showing an exemplary thermodynamic cycle of the ORCHID and deviation from ideal gas of the volumetric properties in the dense vapor and supercritical thermodynamic region in terms of $1 - Z$, where $Z = Pv/RT$. The asterisk which is located along the isentropic expansion in the nozzle represents the thermodynamic state at the nozzle throat. 16
2.4 Results of the thermodynamic analysis for the nozzle experiment: required input thermal power $\dot{Q}_{\text{in}}$ against sound speed in the nozzle throat c_{TH}, for all the candidate WF's of Table 2.1. Fig. a includes all the working fluids considered in the analysis and with a boxed area shown in greater detail in Fig. b. The line in Fig. b identifies the nominal operating load $\dot{Q}_{\text{in}}$ limit, i.e., 370 kW_{th}. 19
2.5 Results of the thermodynamic analysis for the nozzle experiment: maximum WF temperature T_1 against sound speed in the nozzle throat c_{TH}, for all the candidate WF's of Table 2.1. The line identifies the T_1 limit, i.e., 320 °C. . . . 20
2.6 $T - s$ diagram of Siloxane MM, showing the ORCHID thermodynamic cycles during nominal operation of the two TS's. a: nozzle TS in operation (see Table 2.6 for the state-points details), b: turbine TS in operation (see Table 2.7 for the state-points details). 23

3.1 Schematic Layout of the High Speed Lab. showing the main zones. A: ORCHID Lab., B: Thermal Oil Boiler, C: ORCHID Air Coolers, D: HSL Air Coolers and E: Combustion Lab. 28
3.2 Detailed view of the space allocated for the ORCHID Lab. within the High Speed Lab., i.e., detailed view of what is indicated as zone A in Fig. 3.1. The main components of the optical measurement system are also shown, i.e., the LASER, mirrors, and screen, as well as the optical path (blue dashed line). . . 29
3.3 Schematic assembly of the ORCHID set-up, showing the test room and the proposed location of the workstation. 31

4.1 Detailed process flow diagram of the ORCHID facility including the main control loops of the control system (in red). The symbols adopted to represent the latter are the standardized symbols for P&I diagrams 41
4.2 Detailed process flow diagram of the ORCHID facility, including the measurement stations (in red). 45

List of Tables

2.1 Main information about the considered working fluids. 13
2.2 Design Constraints and Assumptions used in the thermodynamic analysis of the nozzle TS. 14
2.3 Results of the thermodynamic analysis for the nozzle experiment, and for the selected WF's. 20
2.4 Design Constraints and Assumptions used in the thermodynamic analysis of the turbine TS. 21
2.5 Results of the thermodynamic cycle calculation related to turbine-testing operation, limited to candidate WF's (see Table 2.1) allowing to reach a cycle net thermal efficiency of the order of 20%. 22
2.6 Operating conditions for the nozzle TS thermodynamic cycle, see also Fig. 2.6. The data for the WF siloxane MM are those to be used to size all the BoP components, i.e. for design purposes. The data for the other WF's have to be considered for verification purposes. 24
2.7 Operating conditions for the turbine TS. The data for the WF siloxane MM are those to be used to size all the BoP components, i.e. for design purposes. The data for the other WF's have to be considered for verification purposes. 25

3.1 Design input for the primary heat exchanger (PHX), the regenerator (REG) and the condenser (COND). The considered HTF is Therminol 66. 34
3.2 Design inputs of the System Pump (with siloxane MM as the working fluid) . . 36

4.1 Measurement stations description and instruments requirements, considering MM as the working fluid and the nozzle experiment only (process data from Table 2.6). 44

Chapter 1

Introduction

1.1 Background

Small-scale and decentralized systems for the conversion of thermal energy are becoming more attractive in the world energy scenario, and Organic Rankine Cycle (ORC) turbo-generators are amongst the most promising technologies used in such applications [10]. However, there are still several issues that prevent their widespread use when operating within the range of a few to tens of kW_e (cost, efficiency, scalability, etc.). One of the major challenges is the miniaturization of the expander, the core component of the ORC unit. A turbine is arguably the best option for the expander, because of efficiency, possibility of expanding the fluid over a large pressure ratio, and reliability. It also does not need any internal lubrication, which is the case for volumetric expanders. The design of efficient and reliable mini-turbines is indeed a daunting engineering problem for two main reasons: limited knowledge on the fluid dynamics of small-scale turbines expanding non-ideal highly compressible fluids (e.g., uncertainty about the accuracy of turbulence models, effect of roughness on turbine fluid dynamic losses, etc.), and the lack of validated design methods or tools (for instance, methods for the selection of the best geometrical configuration of the turbine, loss models, CFD codes, etc.). This technological challenge can only be addressed with experimental studies, similarly to what has been done in the past for the realization of high-performance steam and gas turbines. Similar research efforts are nowadays needed to meet the current challenges posed by the design of mini-ORC turbo-expanders, i.e., in the power range of 10 kW_e.

To this purpose, a new experimental facility capable of continuous operation is being designed and built at the Aerospace Propulsion and Power (APP) Lab of the Delft University of Technology. The name of the set-up, **O**rganic **R**ankine **C**ycle **H**ybrid **I**ntegrated **D**evice (ORCHID), is due to the fact that it consists of a single Balance of Plant[1](BoP) in which an organic fluid is circulated to realize a Rankine thermodynamic cycle, as shown by the simplified Process Flow Diagram (PFD) of Fig. 1.1. Two different test sections (TS's) are closely *integrated* in this BoP, and they can be alternatively fed and used, making the set-up *hybrid*: one TS is a supersonic nozzle with optical access to perform Non-Ideal Compressible Flow Dynamics (NICFD) experiments, while the other TS allows for the performance testing of mini-ORC turbines. The realization of such an experimental facility is funded by two research projects granted by the Dutch Technology Foundation (STW) and by the companies Dana-Spicer Corp. (US) andRobert Bosch GmbH (DE).[2]. The objectives of the projects pertain to the development of mini-ORC turbogenerators for heat recovery from long-haul truck diesel engines, (see the web page of the CC Powertrain project) and small ORC Concentrated Solar Power systems for zero-energy buildings (see the web page

[1]The BoP consists of all infrastructural components of the set-up with the exception of the two test sections.

[2]The STW projects are: i) "Mini-ORC Turbogenerator for Combined-Cycle Powertrains" (grant # 12811), and "Solar ORC Turbogenerator for Zero-Energy Buildings" (grant # 13385).

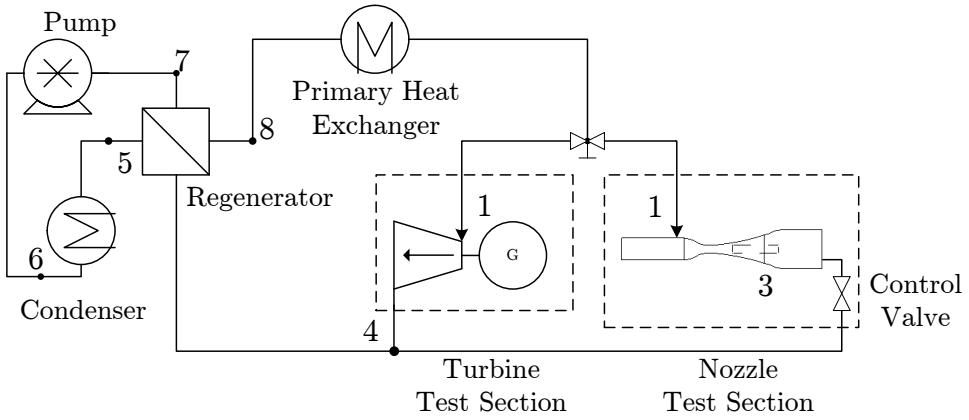

Figure 1.1: Simplified process flow diagram of the ORCHID facility.

of the Mini Solar ORC project).

This report presents the conceptual and preliminary design and analysis of the BoP. The BoPs primary role is to provide a stable and controlled mass flow rate of the working fluid (WF) vapor, at the thermodynamic conditions selected by the operator for the experiment, at the inlet of the TS being used, i.e., at 1 in the PFD of Fig. 1.1. The BoP should be flexible enough to accommodate a number of WFs and the different operating conditions required by the two test sections. This report describes:

- the methodologies developed and applied to define (i) the working fluids suitable for the experiments, (ii) the selected configuration, and (iii) the technical requirements and constraints;
- the results obtained, i.e., a set of design specifications usable as input for the detailed design. These are intended as a basis for discussion with the consulting and engineering company that will be selected to support the P&P research group in the realization of the ORCHID set-up.

The preliminary design and analysis of the test sections is not treated in this document, but will be presented in a follow-up report.

1.2 Motivation

The experiments conducted within the framework of this research program will allow to attain the following objectives:

1. verify the available theoretical body pertaining to Non Ideal Compressible Fluid Dynamics (NICFD), [11, 21, 39, 19, 30, 18] and validate the related thermodynamic models [14, 12] and CFD codes [13, 20];
2. validate the existing – and/or develop novel – semi-empirical correlations, performance estimation methods, and preliminary design methodologies for small-ORC turbines, i.e., in the power range of 10 kW_e; [28, 32, 8] and
3. prove the technical feasibility of high-efficiency ORC power systems for distributed generation in the 10 kW_e power range, by demonstrating a net thermal cycle efficiency of approximately 20%.

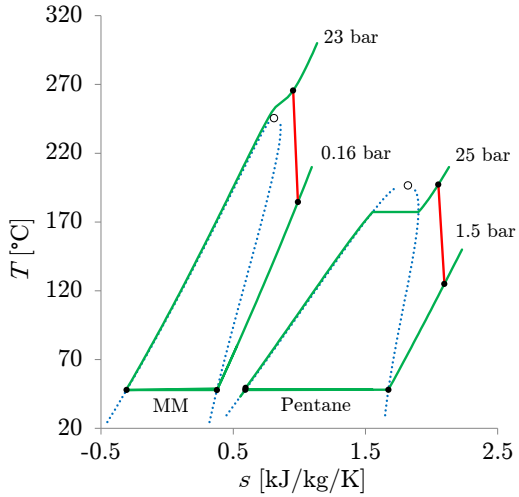

Figure 1.2: $T - s$ diagram of siloxane MM and pentane showing the state points of two possible thermodynamic Rankine cycles of interest for experiments with the ORCHID set-up.

In order to achieve these concurrent objectives, conceptually different experimental facilities are required, namely, a setup which allows to investigate the gas dynamics of dense vapors in NICFD experiments (objective 1), a bench to test turboexpanders performance (objective 2), and a small modular ORC system to prove the downscaling potential of the technology (objective 3). Furthermore, in order for the results to be also of practical use for system and component design, the facility should be able to work with a variety of working fluids and of thermodynamic regions typical of the envisaged applications [10]. This, in turn, calls for the ability of the set-up to operate within a comparatively large range of pressure and temperature levels. In order to illustrate the diversity of the thermodynamic cycles of interest, Fig. 1.2 shows two exemplary thermodynamic cycles that could be realized with the ORCHID set-up. By adopting the heavier molecule WF, i.e., siloxane MM, it is possible to realize a supercritical cycle at a pressure which is lower than the evaporation pressure of the pentane cycle. Also, the two working fluids feature a large difference in terms of condensing pressure for the given temperature.

1.3 The Setup Concept

The ORCHID setup has been conceived to cope with the demanding requirements outlined in the previous section. Even though similar facilities have been pioneered decades ago in the field of Aerodynamics [34, 33, 6], investigations with organic vapors require the conception of an innovative set-up able to operate at high pressure and temperature and compatible with the use of different working fluids. Regarding the ORCHID set-up, the main conceptual design choices that were taken are:

1. to realize one single BoP which is able to alternatively supply both the test sections with working fluid at set operating conditions. This implies a number of design challenges, but offers advantages that are deemed preponderant with respect to the construction of two distinct facilities. For instance, there are economic advantages in concentrating the financial effort on the realization of one set-up which can then be, e.g., equipped with more advanced instrumentation; and

2. to adopt a closed loop configuration, which is deemed the superior solution in relation to the research objectives, since it permits to

a) reproduce the operating conditions of a (downscaled) state-of-the art ORC power system,

b) avoid limitations on the testing time: once the setup reaches steady operation continuous measurement campaigns are possible,

c) avoid critical issues concerning the use and control of high-temperature fast acting valves, and

d) reduce the complexity of interpretation of experimental data, since the boundary conditions given by the BoP components are stable throughout the test.

Other setups for ORC-technology-related research have been recently presented, such as the TROVA built at Politecnico di Milano - Italy, [35] and the Gas Cycle Facility built at Universität Paderborn - Germany [22]. However, the conceptual design choices illustrated here are different from those of the TROVA and the Gas Cycle Facility, thus making the ORCHID a novel and unique experimental facility [24].

1.4 Design Procedure

As the first step in the design process, the thermodynamic analysis defines the configuration of the set-up, the possible working fluids for each test section, and the operating specifications for the design of the main components. In order to enhance the operating flexibility of the facility and to guarantee the possibility to use different working fluids, the BoP has then been preliminarily sized with respect to the most demanding experimental conditions in terms of WF mass flow rate, required thermal power input, and thermal loads of the heat exchangers. Moreover, despite the TS's integration into the same BoP being relatively straightforward, their compatibility of operation needed to be assessed due to their different design requirements. For instance, as discussed in the following, on the one hand the thermal load needed for the operation of the nozzle TS can be one order of magnitude larger than that required for turbine testing. On the other, the turbine TS is much more demanding in terms of cycle temperature and pressure. This diversity implies that the sizing of the main components of the set-up has to be carried out by considering simultaneously the design specifications of both the TS's.

1.5 Report Structure

This report is structured as follows. Ch. 2 describes the methodology developed to obtain the thermodynamic cycle design and analysis, and how such methodology allowed to identify the most demanding WF in terms of operating conditions. Based on these results, requirements and specifications for all the components of the BoP are illustrated in Ch. 3. The requirements and specifications of the Data Acquisition (DAQ) and control system are discussed in Ch. 4.

Chapter 2

Thermodynamic Analysis of the BoP: Nominal Operating Conditions

2.1 Cycle Configuration

The primary energy source of the ORCHID will be electricity because of its inherently simple regulation and control, together with less strict safety and hazard requirements. Furthermore, from the point of view of its thermodynamic quality or exergy content, the thermal equivalent of electricity is a source at infinite temperature [29]. The goal of the thermodynamic cycle implemented in the ORCHID is the conversion of part of the available thermal energy into kinetic energy of the dense vapor flow (for the nozzle experiment) or mechanical power (for the turbine experiment). Increasing the efficiency of this conversion process is of great interest, in particular for turbine testing. It is known from textbooks on applied Thermodynamics [29] that, in order to maximize the efficiency of the cycle, the input thermal power should be transferred from the source to the cycle itself at the highest possible temperature. In the practice of Rankine cycle-based power systems, this temperature is limited to values lower than 700 °C by the compatibility with materials (e.g., those used in the furnaces piping), thus introducing what is typically the largest thermodynamic loss of any such thermal power conversion process. In ORC systems and thus also in the ORCHID case, as detailed in the following (see §2.3), this limit must be further lowered to values under 400 °C due to the thermal stability limits of organic working fluids.

A common solution to increase the average temperature at which thermal power is introduced into the cycle is the *internal regeneration*, and the choice of adopting a regenerator is, in general, the result of a thermo-economic optimization process. When a so called *dry fluid* is used as the WF,[1] the regenerator can be a surface heat exchanger, making the system layout much simpler with respect to, e.g., the regeneration based on the extraction of steam from the turbine at different pressure levels, as done in steam power plants. For this reason, all commercial ORC power systems for the conversion of high-temperature energy sources adopt this configuration[2] [25, 10].

Concluding, the most attractive arrangement for the ORCHID set-up is deemed to be a regenerative cycle configuration since:

- It allows to attain higher cycle efficiency; and

[1] Dry fluids are those for which the curve bounding the liquid-vapor coexistence region displays a positive slope of the saturated vapor branch in the $T - s$ diagram, as shown in Fig. 1.2. For such WF's, an expansion process starting from saturated vapor conditions proceeds towards superheated (i.e., *dry*) vapor states, contrary to what happens for wet fluids such as water.

[2] More complicated analyses might be needed if considering ORC systems designed for different applications such as, notably, heat recovery from sensible heat thermal sources [3, 4].

- This arrangement closely resembles that of state-of-the-art high temperature ORC power systems, making the envisaged experimental results of more immediate interest.

Fig. 2.1 shows the detailed Process Flow Diagram (PFD) of the set-up configuration with both primary test sections in parallel (the primary TS's are enclosed in dotted rectangles). The BoP is made up of the following components: pump, primary heat exchanger (PHX), regenerator, condenser and auxiliary components like tanks and valves. An exemplary $T-s$ diagram of the thermodynamic cycles realized in the ORCHID is depicted in Fig. 2.2 and, with reference to the state points shown, the processes undergone by the working fluid are as follows:

- Thermodynamic state 1 (entrance of the test sections) corresponds to the beginning of the expansion process which, depending on the experiment being carried out, proceeds toward

  - thermodynamic state 3 in case of expansion in the nozzle (i.e., nozzle TS in operation). This process (1-3), is assumed isentropic in this preliminary analysis. This is followed by the dissipation process in a valve (3-4), whereby the kinetic energy of the supersonic flow at the nozzle outlet is throttled in the back-pressure valve downstream of the receiver tank;

  - thermodynamic state 4 in case of expansion in the turbine (i.e., turbine TS in operation). This process (1-4), assumes an isentropic turbine efficiency equal to 70 % in this preliminary analysis.

- From thermodynamic state 4 to 5 vapor flow is cooled down to preheat the liquid stream at the pump outlet (process 7-8);

- From thermodynamic state 5 to 6 the working fluid condenses by transferring energy as heat to the cooling water circuit;

- From thermodynamic state 6 to 7 the pump pressurizes the condensate to the evaporation (sub-critical cycle) or primary heater (super-critical cycle) pressure. This process is hardly noticeable in a $T-s$ diagram because the associated temperature increase is negligible;

- From thermodynamic state 7 to 1 the working fluid temperature is increased in the PHX, by extracting thermal power from an another fluid loop which, in turn, is heated by the primary source. In this case the primary source is electricity use to heat thermal oil (electrical oil heater). The conditions required by the experiment are thus reached, and this process also closes the thermodynamic cycle.

AC: Air Coolers
BD: Burst Disk
BPV: Buoyant Plug Valve
BT: Buffer Tank
CHX: Condenser Heat Exchanger
CV: Check Valve
DT: Dump Tank
D1...n: Drain Valves
FDP: Flow Damper
LS: Liquid Separator
NCV: Nozzle Control Valve
P: Pump
PB: Pump Bypass
PHX: Primary Heat Exchanger
PIV-AP: PIV- Access Point
PIV-F: PIV-Filter
RV: Relief Valve
RHX: Regenerator Heat Exchanger
SC: Settling Chamber
TOH: Thermal Oil Heater
TSC: Test Section Channel
TB: Turbine Bypass
TMV: Turbine Main Valve
VP : Vacuum Port
VV1...n :Vacuum Pump Circuit Valves
V1...n: Ball Valves

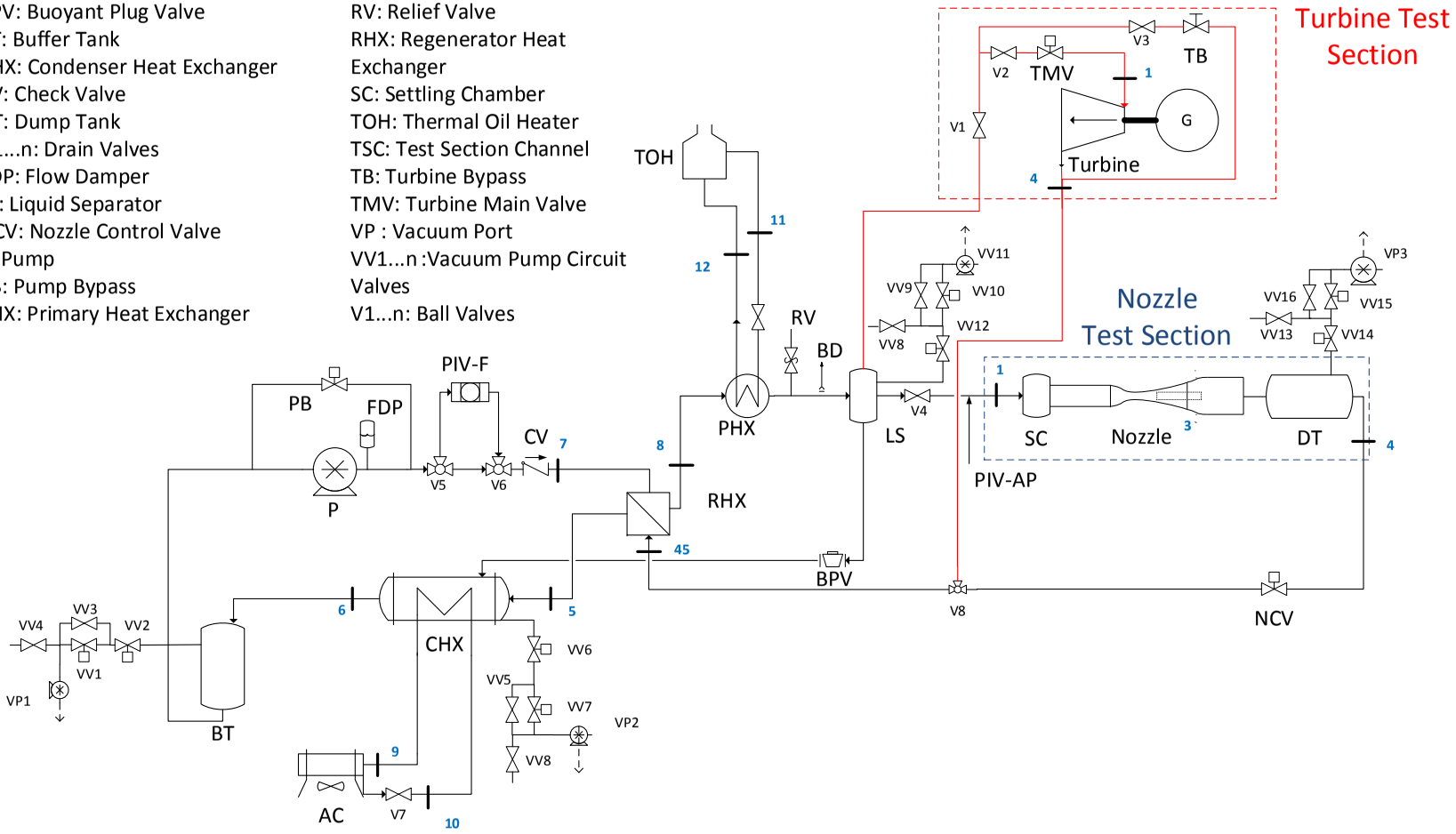

Figure 2.1: Detailed process flow diagram of the ORCHID facility.

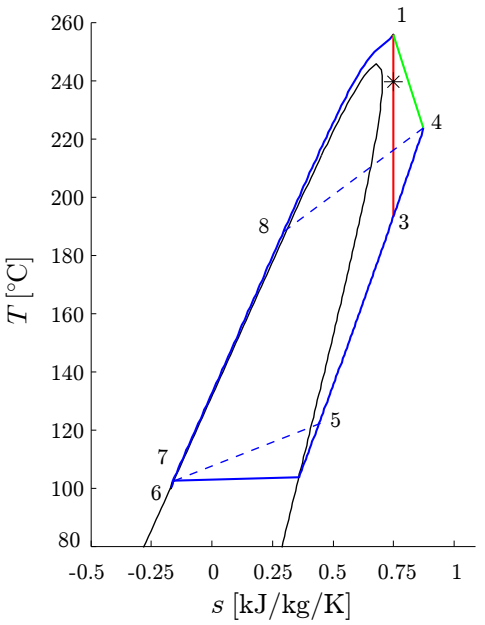

Figure 2.2: Exemplary thermodynamic cycles in the $T - s$ diagram of the working fluid (siloxane MM in this case). The blue lines represent the processes in common to the operation of both TS's. The red line shows the expansion process from supercritical conditions if the nozzle TS is in operation (the cycle encompasses the state points $6{-}7{-}8{-}1{-}*{-}3{-}4{-}5$). The asterisk highlights the thermodynamic state in the throat of the nozzle. The green line shows the expansion process if the turbine TS is in operation (the cycle encompasses the state points $6-7-8-1-4-5$). Numbered thermodynamic states refer to conditions at components interfaces as reported in the process flow diagram of Fig. 2.1.

The thermodynamic state points of the cycle can be calculated starting from selected main operating parameters (pressures and temperatures) using a standard textbook method resulting from the application of mass and energy conservation to each process. State-of-the-art thermodynamics models, implemented in an in-house software library, have been used to determine the thermophysical properties of the considered WF's [15, 26].

The cycle details depend on the TS being analyzed, because each TS has its own design constraints, e.g., in terms of thermal energy input, condensing pressure and maximum temperature. For this reason, during the preliminary analysis of the BoP, the nozzle and the turbine TS's have been considered independently.

2.2 Working fluids

As anticipated, the ORCHID set-up must be able to operate with a wide range of WF's of interest in ORC technology practice. A list of these compounds, which are the candidates considered in this analysis, is collected in Table 2.1. They belong to different classes, namely, *hydrocarbons*, *organofluorines*, and *siloxanes*[12]. Table 2.1 shows the critical temperature and pressure T_{CR} and P_{CR}, the boiling temperature T_{boil}, and the thermal stability temperature limit of the fluid T_{TD} (thermal degradation temperature), i.e., the temperature above which the WF is subjected to fast thermal decomposition reactions leading to irreversible degradation. The selected ORC fluids tend to thermally degrade at high temperatures, and these thermal decomposition reactions are strongly accelerated by the presence of oxygen, humidity, and other contaminants such as, e.g., the products coming from the oxidation of the containing materials. Other important factors playing a role in these phenomena are the containment material and the dynamics of heating (e.g., fast temperature oscillations

Table 2.1: Main information about the considered working fluids.

Siloxanes	T_{CR} [°C]	P_{CR} [*bar*]	T_{boil} [°C]	T_{TD} [°C]
D_4	313.3	13.3	175.3	≈ 350 [14]
D_5	346.0	11.6	210.9	≈ 350 [14]
D_6	372.6	9.61	245.0	≈ 350
MM	245.6	19.4	100.2	≈ 300 [38]
MDM	290.9	14.2	152.5	≈ 350 [14, 9]
MD_2M	326.2	12.3	194.4	≈ 350 [14]
MD_3M	355.2	9.4	229.9	≈ 350
MD_4M	380.1	8.8	260.7	≈ 350
Hydrocarbons				
Toluene	318.6	41.3	110.6	≈ 400 [23, 37, 2]
Pentane	196.5	33.7	36.1	≈ 270 [27]
Cyclopentane	238.5	45.1	49.3	≈ 300 [17]
Perfluorocarbons (PFC's)				
PP2	212.9	20.2	76.0	≈ 400 [16]
PP80	233.97*	16.85*	103.2	≈ 400
PP90	256.85*	16*	125.1	≈ 400
Hydrofluorocarbons (HFC's)				
R245fa	154.0	36.5	15.1	≈ 260 [1, 40]

*Estimated by thermodynamic predictive models.

vs long term steady exposure). However, only few studies have been published on this topic, and both the testing methodologies and the gathered data are non homogeneous and difficult to compare [9, 31, 2]. As a general consideration, it is worth highlighting that the ORCHID setup is conceived to perform experimental investigations at thermodynamic conditions close to the expected thermal decomposition limit of the fluids.

2.3 Main Design Constraints

Several important constraints common to both the TS's have been identified, as discussed in the following. The maximum available electric power for the set-up is equal to approximately 400 kW_e. This value has been determined based on local technical constraints on the power cabin, and by the need of limiting the investment and operating costs. Furthermore, being known from the literature that the power required to start-up conventional supersonic closed-loop facilities is higher than that required for steady state operation [34], the nominal design load of the PHX $\dot{Q}_{in,max}$ has been limited to 370 kW_{th}.

After a dedicated investigation about the maximum thermal power input, which involved experts consultancy and interactions with manufacturers, it has been preliminary decided to adopt an electric oil heater as the thermal power source of the ORCHID set-up (see §3.3 for details). The thermal input to the ORCHID will thus be provided through an intermediate Heat Transfer Fluid (HTF) loop where a thermal oil is (i) heated up by heating rods, (ii) circulated through the PHX where it transfers thermal power (being cooled) to the ORC working fluid (which is being heated up), and (iii) returned to the electric heater. The main thermodynamic implication deriving from the adoption of this intermediate oil loop is that the maximum cycle temperature (i.e., the maximum temperature of the WF, $T_{WF,max}$) is limited by the thermal stability temperature limit of the HTF. In particular, for thermal oils commonly used in industrial high-temperature applications such a limit is about 340-350 °C. Therefore, assuming an approach temperature difference of 25 °C at the hot end of the PHX, a limiting value of $T_{WF,max} = 320$ °C is estimated.

The limit imposed on $T_{WF,max}$ is not expected to affect the ORCHID potential in testing simpler molecule-WF's, such as those used in low temperature ORC applications. On the other hand, some experiments of interest involving high temperature WF's will not be

achievable with this set-up configuration. However, this limit is not much lower than the thermal stability temperature limit of the envisaged test fluids, as detailed in the previous section.

Finally, the maximum WF pressure in the system is set to 25 bar. This limit has been selected due to a preliminary investigation about the pressure rating of suitable equipment, i.e., most notably, the high temperature welded plate heat exchangers (see §3.5).

Summarizing, the design constraints which are considered in all the analyses presented in the following are:

- the maximum operating load of the PHX is $\dot{Q}_{\mathrm{in,max}} = 370\ \mathrm{kW_{th}}$;
- the maximum ORC fluid temperature is $T_{\mathrm{WF,max}} = 320\ ^{\circ}\mathrm{C}$. The maximum temperature is expected to occur at the outlet of the PHX, and is close to T_1 (depending mainly on the thermal losses from the PHX to the nozzle TS). The constraint that is thus enforced in the following analyses is $T_1 < T_{\mathrm{WF,max}} = 320\ ^{\circ}\mathrm{C}$. Notably, for the fluids for which $T_{\mathrm{TD}} < 320\ ^{\circ}\mathrm{C}$ (see Table 2.1), the maximum WF temperature is lowered and assumed to be equal to the thermal degradation temperature, i.e., $T_{\mathrm{WF,max}} = T_{\mathrm{TD}}$; and
- the maximum ORC fluid pressure is $P_{\mathrm{WF,max}} = 25$ bar. The maximum pressure is expected to occur at the outlet of the pump, and is thus close to P_1 (depending mainly on the pressure losses from the PHX to the nozzle TS). The constraint that is thus enforced in the following analyses is $P_1 < P_{\mathrm{WF,max}} = 25$ bar.

2.4 Design of the Supersonic Nozzle Test Section

Assumptions

As anticipated in §1.2, the main purpose of this testing system is to perform fundamental studies on dense and supercritical vapor flows (i.e., NICFD experiments). Several design constraints and a number of more general assumptions have to be considered, beside those detailed in §2.3, in order to meet the required experimental conditions. These are collected in Table 2.2, and are now described (following the same order proposed in the table). These data are thus used to perform the thermodynamic analysis which, together with its results, is discussed in the next two subsections. The first design constraint comes from the need

Table 2.2: Design Constraints and Assumptions used in the thermodynamic analysis of the nozzle TS.

	Variable	Value
nominal thermal power (max), see §2.3	$\dot{Q}_{\mathrm{in,max}}$	370 $\mathrm{kW_{th}}$
WF temperature (max), see §2.3	$T_{1,\mathrm{max}}$	max(320 °C, T_{TD})
WF pressure (max), see §2.3	$P_{1,\mathrm{max}}$	25 bar
inlet reduced pressure	$P_{1,\mathrm{R}}$	>1
nozzle Mach number (out)	M_{min}	1.8
condenser pressure	P_6	1.0 bar
throttling valve pressure drop	ΔP_{TV}	1.0 bar
nozzle discharge pressure	P_3	2.1 bar
cooling water temperature (in)	$T_{\mathrm{H2O,in}}$	20 °C
PHX temperature diff. @ pinch point	$\Delta T_{\mathrm{PP,PHX}}$	25 °C
Regenerator temperature diff. @ pinch point	$\Delta T_{\mathrm{PP,REG}}$	20 °C
Heat exchangers pressure losses	ΔP_{HX}	max(1.0 % P_{in}, 0.1 bar)
Pump hydraulic efficiency	$\eta_{\mathrm{is,PUMP}}$	50 %
Mechanical transmission efficiency	$\eta_{\mathrm{m,TRANSM}}$	92 %
Electric machine efficiency	$\eta_{\mathrm{e,EM}}$	96 %

of obtaining a supercritical flow in the TS. To this end, the reduced pressure[3] at the inlet of the nozzle (i.e., at the beginning of the expansion process) $P_{1,\mathrm{R}}$ must be greater than 1. It is furthermore required that the Mach number at the outlet of the nozzle is comparable to the Mach number at the stator outlet of high-temperature ORC turbines. For this reason, the minimum Mach number at the outlet of the nozzle, i.e. M_{min}, has been set to a value of 1.8. Another design constraint is imposed regarding the nozzle discharge pressure. As mentioned, avoiding air-intakes in the set-up is important to avoid the risk of WF thermal decomposition. For this reason, the lower pressure in the system P_6, i.e., the one established in the condenser (nomenclature referring to Fig. 2.1), is limited to atmospheric pressure. The throttling valve placed between the nozzle outlet and the condenser inlet (see Fig. 2.1) is intended as a fundamental regulation device, which allows to control the flow conditions in the nozzle. Following a preliminary analysis of this component it is assumed that, during nominal operation, a pressure drop of 1 bar has to be guaranteed across the valve, i.e., $\Delta P_{\mathrm{TV}} = 1$ bar. This constitutes an additional design constraint, which furthermore imposes the nominal operating pressure at the nozzle discharge, i.e. P_3, being $P_3 = P_6 + \Delta P_{\mathrm{TV}}$. The stream of water for the cooling of the condenser is assumed to be available at an inlet temperature of $T_{\mathrm{H2O,in}} = 20$ °C. A number of further assumptions regarding the performance of the BoP components, and the assumed values are taken from common practice encountered in commercial ORC systems. In particular, the performance of the heat exchangers (HX's) is expressed by the minimum temperature difference achieved between the two fluids within the same devices, i.e., the pinch point temperature difference ΔT_{PP}. For PHX the latter coincides with the approach temperature difference at the thermal oil inlet section. The pressure drops within each side of the HX's have been accounted for as a fixed percentage of the relative inlet pressure, or as a fixed absolute value of 0.1 bar, whichever value results larger. Finally, the efficiencies of the components constituting the pump-group are determined by the values given to (i) the pump isentropic efficiency $\eta_{\mathrm{is,PUMP}}$, (ii) the mechanical efficiency of its transmission system $\eta_{\mathrm{m,TRANSM}}$, and (iii) the electrical efficiency of its drive motor $\eta_{\mathrm{e,EM}}$.

Procedure

The procedure for the design of the nozzle test section involves two fundamental variables, namely:

- the reduced pressure at the inlet of the nozzle, i.e. $P_{1,\mathrm{R}}$; and
- the geometrical area of nozzle throat A_{TH}, which is the minimum flow passage area where the flow attains sonic conditions (i.e., chocking conditions).

The relation among $P_{1,\mathrm{R}}$ and A_{TH}, which drives the whole design process, is outlined in the following.

In order to perform the NICFD experiments of interest, a vapor flow at relatively high Mach number must be established in the nozzle TS. The experiment results will be particularly valuable as the thermodynamic conditions of the expanding fluid will be in the so-called dense vapor regime, in turn causing the flow behavior to deviate from that of ideal gas flow, thus belonging the realm of NICFD. As an example, Fig. 2.3 shows the $T - s$ diagram of a possible thermodynamic cycle implemented by the nozzle TS, using siloxane MDM as the WF. The isentropic expansion process depicted in the figure involves non-ideal compressible flow dynamic effects, as it crosses the dense vapor region, i.e., the region where $1 - Z$ is very different from 0 and strongly varies ($Z = Pv/RT$ is the compressibility factor, providing one of the indications of deviation from ideal gas behavior). Stronger non-ideal

[3] To compare different fluids it is common to scale the pressure values to the critical pressure of the fluid. This non dimensional value is called reduced pressure. Thus, the reduced pressure $P_{\mathrm{x,R}}$ of a thermodynamic state x can be evaluated as $P_{\mathrm{x,R}} = \frac{P_{\mathrm{x}}}{P_{\mathrm{CR}}}$, where P_{CR} is the critical pressure of the considered WF.

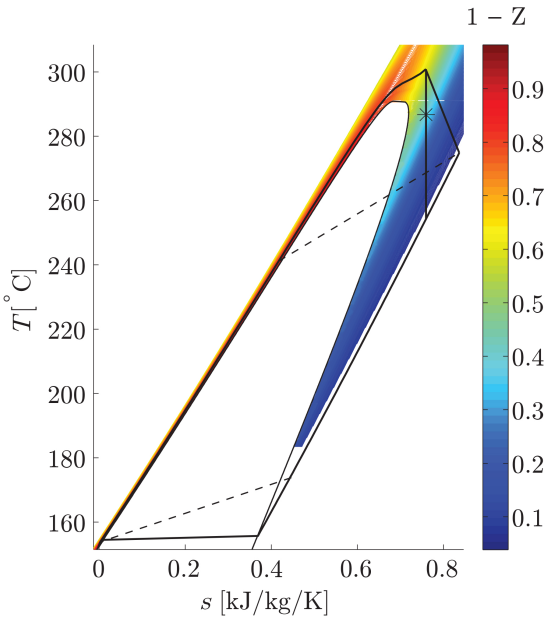

Figure 2.3: $T - s$ Diagram of MDM showing an exemplary thermodynamic cycle of the ORCHID and deviation from ideal gas of the volumetric properties in the dense vapor and supercritical thermodynamic region in terms of $1 - Z$, where $Z = Pv/RT$. The asterisk which is located along the isentropic expansion in the nozzle represents the thermodynamic state at the nozzle throat.

gas dynamic effects,[4] as predicted by the adopted thermodynamic models, are encountered for regions characterized by larger $1 - Z$ values, and operating the nozzle TS in these conditions would allow to achieve the most desirable experimental conditions. In order to achieve this result, one should increase $P_{1,\mathrm{R}}$: the vapor would thus reach increasingly supercritical conditions, and the subsequent expansion process is influenced to a greater extent by non-ideal compressible fluid dynamic effects. Being the nozzle discharge pressure fixed, increasing $P_{1,\mathrm{R}}$ causes an increase in the flow Mach number, which only depends upon the pressure difference across the nozzle.

On the contrary, the throat section A_{TH} does not influence the thermodynamic region of operation of the nozzle. However, since the nozzle is expected to always work in choked conditions, this geometrical parameter determines the mass flow rate circulating in the nozzle and, as a consequence, in the whole set-up. In order to explain this relation, an isentropic expansion process can be assumed in the nozzle from the inlet section, where total conditions are known (i.e., pressure $P_{1,\mathrm{T}}$ and temperature $T_{1,\mathrm{T}}$), to the throat, where sonic conditions are attained (i.e., the flow speed equals the speed of sound c). Accordingly, the system of equations governing the expansion is

$$\begin{cases} s = s(P_{1,\mathrm{T}}, T_{1,\mathrm{T}}) \\ h_{\mathrm{S,TH}} = h_{1,\mathrm{T}}(P_{1,\mathrm{T}}, T_{1,\mathrm{T}}) - \dfrac{1}{2}c^2(h_{\mathrm{S,TH}}, s) \\ \dot{m} = \rho_{\mathrm{S,TH}}(h_{\mathrm{S,TH}}, s) \cdot c(h_{\mathrm{S,TH}}, s) \cdot A_{\mathrm{TH}} \ , \end{cases} \tag{2.1}$$

where s is the specific entropy, and the subscript "S,TH" indicates static conditions in the throat section. The first equation in the system (2.1) expresses the isentropic nature of

[4] A more rigorous approach would consider the fundamental derivative of gas dynamic Γ, see e.g. Ref. [11], but for design described here and the desired level of accuracy, the approach based on the compressibility factor Z is deemed sufficient

the process model,[5] the second the conservation of total enthalpy (i.e., energy balance in an adiabatic system without work extraction), and the third the continuity equation. The system of equations (2.1) clarifies the relation existing among the mass flow rate flowing in the nozzle $\dot{m}$, the thermodynamic properties at the expansion inlet, and the flow passage area A_{TH} in the throat section. In particular, by considering the thermodynamic conditions as fixed, it is important to note that the relation between $\dot{m}$ and A_{TH} reduces to a linear proportionality with constant coefficient.

It is thus relevant that increasing $\dot{m}$ necessitates a proportional increase in the input thermal power, as expressed by

$$\dot{Q}_{\mathrm{in}} = \dot{m}\ (h_{1,\mathrm{T}} - h_{8,\mathrm{T}}) \propto \dot{m}\ h_{1,\mathrm{T}}\ . \tag{2.2}$$

In the proportionality relation of (2.2), it is further considered that the conditions at thermodynamic state 8 (nomenclature referring to Fig. 2.1) are relatively insensitive to variations in state 1, given the assumptions collected in Table 2.2.

All the other thermodynamic state points of the ORC are determined by applying standard procedure for thermodynamic cycle calculation based on the conservation of mass and energy.

Summarizing, under the assumption of choked nozzle, the system of equations (2.1) and equation (2.2) allow to conclude that:

- $\dot{m}$ is not influenced by the nozzle discharge pressure,
- $\dot{m}$ is directly proportional to A_{TH},
- an increase in the inlet pressure $P_{1,\mathrm{R}}$ causes an increase of $\dot{m}$ as a result of the increase in both the density and the speed of sound in the nozzle throat,[6]
- any increase of $\dot{m}$ causes $\dot{Q}_{\mathrm{in}}$ to increase as well.

The following section details how the above outlined trade-offs have been tackled to define the nozzle TS design.

Results

Results are obtained from the analysis conducted by means of (i) the in-house code *ORC Virtual Prototyping Environment (VPE) v1.0* [5] implementing the problem formulation presented in the previous subsection (a lumped parameters model, or 0-D approach is adopted for all the ORC components), and (ii) an in-house CFD software tool to study the nozzle TS flow-field (the detailed results of this study will be presented in a dedicated follow-up report). The first important finding is that the constraint on $\dot{Q}_{\mathrm{in}}$ is the most stringent affecting the nozzle TS. In order to limit the required thermal power, while fulfilling the constraints and the assumptions collected in Table 2.2 for all the candidate WF's, three fundamental design choices are identified as necessary, i.e.

1. The value of the nozzle throat area A_{TH} must be minimized. The selected value is 200 mm^2 which, since the nozzle has a rectangular section,[7] corresponds to a throat height of 10 mm and a width of 20 mm. This follows from (i) the necessity of providing

[5] for the scope of the analysis, viscous effects in the nozzle are negligible.

[6] The speed of sound may not be a strictly growing function of the pressure in case the so-called BZT fluids are considered, for which the fundamental derivative of gas dynamics $\Gamma \equiv 1 + \frac{\rho}{c}\left(\frac{\partial c}{\partial \rho}\right)_s = \frac{v^3}{2c^2}\left(\frac{\partial^2 P}{\partial v^2}\right)_s$, might become negative in a finite thermodynamic region. [36] Even if the use of BZT fluids in ORC power systems is foreseen to have a potential interest, [7] and some of the considered WF's feature a BZT region, [12] this option is not considered at the present stage of the research.

[7] This is related to the optical measurement technique envisaged, i.e., PIV, due to unwanted distortions of the laser light sheet in case it has to cross a curved window.

physical dimensions of the TS large enough to allow for the use of flow visualization and measurement techniques (e.g., Schlieren and PIV), with a sufficient level of accuracy; and (ii) the need of minimizing the influence of the Boundary Layer (BL) and to avoid BL-induced blocking effects during the experiments.

2. The value of the nozzle inlet pressure has to be limited to a slightly supercritical value, i.e., $P_{1,\mathrm{R}} = 1.1$ for all the considered WF's.[8]

3. The value of the nozzle inlet temperature, T_1, has to be such as to prevent condensation during the expansion in the nozzle. Notably, T_1 is defined as:

$$T_1 = T(P_1, s^* + \Delta s) \tag{2.3}$$

where s^* is the maximum specific entropy of the saturated vapor in the pressure range involved in the nozzle expansion process ($P_1 \rightarrow P_3$) and Δs represents a safety margin with respect to the saturation curve. In order to define this parameter consistently for each candidate WF's, Δs is assumed in the analysis herein described equal to 5% of s^*.

The results of the thermodynamic cycle analysis, conducted under the assumptions collected in Table 2.2, further integrated by the design choices reported above, are discussed in the following. First of all, it is confirmed that $\dot{Q}_{\mathrm{in}}$ is significantly affected by the WF thermodynamic properties, as shown by Fig. 2.4, where this quantity is plotted against the sound speed in the nozzle throat c_{TH}. c_{TH} is adopted as design parameter since (i) it is a property suited to provide a comparison between the WF's given its relations with the fluids molecular complexity, and (ii) it has a relation with the expansion process, as expressed by the system of equations 2.1. The general trend clearly depicted in Fig. 2.4 is that more complex WF's tend to have lower c_{TH} values which, in turn, tend to decrease the needed $\dot{Q}_{\mathrm{in}}$. This result follows from the combination of the variation trends of several interrelated quantities. In addition to the considerations detailed in §2.4, also the shape of the liquid-vapor region is expected to be influential, since different WF's belonging to different families are being compared. For instance, molecular complexity may induce variations in the amount of regenerated thermal power within the different ORC's. The interested reader is referred to the work of Invernizzi [25] for a detailed description of these aspects, which are beyond the scope of this report.

Among the candidate WF's presented in Table 2.1, only those for which the needed $\dot{Q}_{\mathrm{in}}$ does not exceed the limit of $\dot{Q}_{\mathrm{in}} < 370$ kW$_{\mathrm{th}}$ has been further considered, and it results that all the candidate siloxanes and PFCs can be tested with the current constraints, with siloxane MM being the only exception, as shown in Fig. 2.4. However, since MM is one of the most promising fluids for small-scale ORC power systems, the ORCHID setup should allow to perform nozzle experiments also with this WF. Considering that MM requires a $\dot{Q}_{\mathrm{in}}$ which exceeds the limitation only slightly under the adopted assumptions, the use of MM is accounted for, but limited to subcritical experiments. In other words, this fluid is considered in the following, but the nozzle inlet pressure is reduced with respect to all the other WF's, down to the sub-critical value of $P_{1,\mathrm{R}} = 0.95$, which allows the constraint on $\dot{Q}_{\mathrm{in}}$ to be fulfilled (with $\dot{Q}_{\mathrm{in}} = 352$ kW$_{\mathrm{th}}$).

Secondly, Fig. 2.5 reports the information regarding the maximum WF temperature during the nozzle experiments. Similarly to the previous analysis based on the $\dot{Q}_{\mathrm{in}}$ limit, the limit on $T_{\mathrm{WF,max}}$ (e.g., on T_1, see §2.3) determines the rejection of several other WF's, namely, D_5 ($T_1 = 353$ °C), D_6 ($T_1 = 380$ °C), $\mathrm{MD}_2\mathrm{M}$ ($T_1 = 334$ °C), $\mathrm{MD}_3\mathrm{M}$ ($T_1 = 363$ °C), and $\mathrm{MD}_4\mathrm{M}$ ($T_1 = 387$ °C).

[8] Notably, this value is in the range of the optimal values as predicted by studies on supercritical ORC power systems.

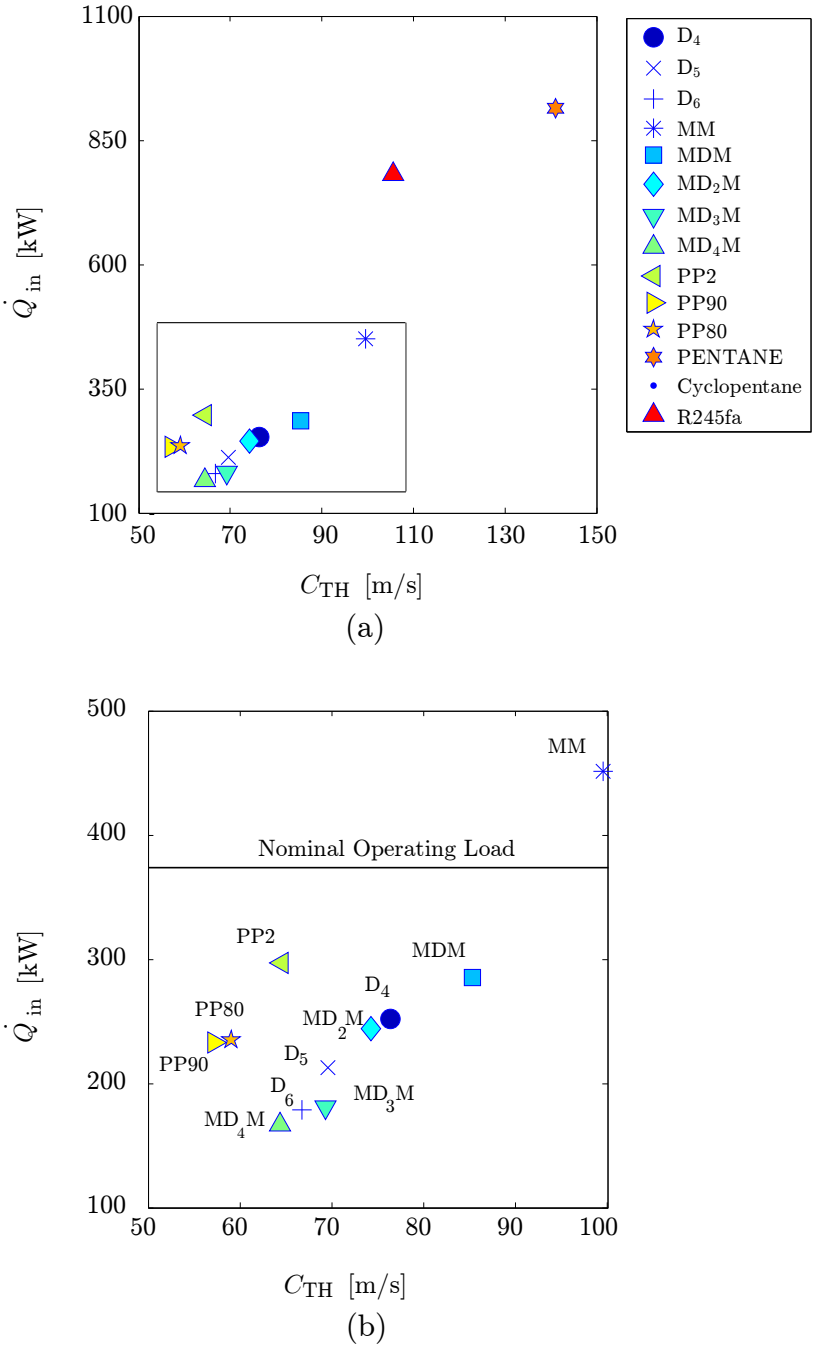

Figure 2.4: Results of the thermodynamic analysis for the nozzle experiment: required input thermal power $\dot{Q}_{\text{in}}$ against sound speed in the nozzle throat c_{TH}, for all the candidate WF's of Table 2.1. Fig. a includes all the working fluids considered in the analysis and with a boxed area shown in greater detail in Fig. b. The line in Fig. b identifies the nominal operating load $\dot{Q}_{\text{in}}$ limit, i.e., 370 kW_{th}.

Summarizing the results, the substances suitable for gas dynamic experiments in the nozzle TS are MM (with $P_{1,\text{R}} = 0.95$), MDM, D_4, PP2, PP80 and PP90. The main results of the thermodynamic analysis are collected, for these WF's only, in Table 2.3, which reports the values of the input thermal power $\dot{Q}_{\text{in}}$, the thermal power exchanged in the regenerator

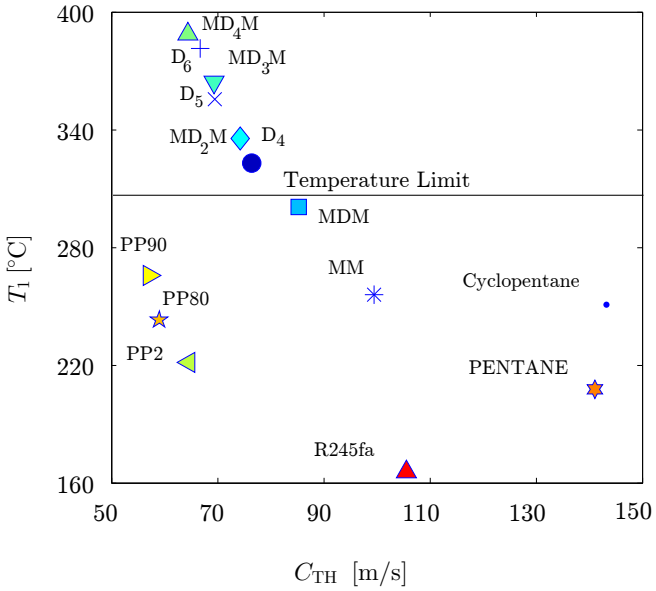

Figure 2.5: Results of the thermodynamic analysis for the nozzle experiment: maximum WF temperature T_1 against sound speed in the nozzle throat c_{TH}, for all the candidate WF's of Table 2.1. The line identifies the T_1 limit, i.e., 320 °C.

$\dot{Q}_{REG}$ and in the condenser $\dot{Q}_{COND}$, the pump electrical power $\dot{W}_{PUMP}$, the temperature and pressure levels a the nozzle inlet T_1 and P_1, the condensing temperature P_6, and the circulating mass flow rate $\dot{m}_{WF}$.

Table 2.3: Results of the thermodynamic analysis for the nozzle experiment, and for the selected WF's.

fluid	$\dot{Q}_{in}$ [kW$_{th}$]	$\dot{Q}_{REG}$ [kW$_{th}$]	$\dot{Q}_{COND}$ [kW$_{th}$]	$\dot{W}_{PUMP}$ [kW$_e$]	T_1 [°C]	P_1 [bar]	T_6 [°C]	$\dot{m}_{WF}$ [kg/s]
MM	352	315	360	9	252	18.4	100	1.6
MDM	291	284	298	7	299	15.6	153	1.5
D_4	260	267	265	6	321	14.7	176	1.6
PP2	302	254	309	8	219	22.7	75	3
PP80	238	250	243	6	241	18.5	100	2.6
PP90	235	254	240	6	264	17.6	124	2.6

2.5 Turbine Test Section

Assumptions

As anticipated in §1.2, the main purposes of this testing system are (i) to experimentally investigate the performance of small ORC turbines, and (ii) to prove the potential of ORC technology in the same power range, i.e., 10 kW$_e$. Several design constraints and a number of more general assumptions have to be imposed, beside those detailed in §2.3, in order to meet the required experimental conditions. These are collected in Table 2.4, and most of them have been described already in Table 2.2. For this reason, only the newly introduced quantities are treated here. These data are thus used to perform the thermodynamic analysis which, together with its results, is discussed in the next two subsections.

Table 2.4: Design Constraints and Assumptions used in the thermodynamic analysis of the turbine TS.

	Variable	Value
nominal thermal power (max), see §2.3	$\dot{Q}_{\text{in,max}}$	370 kW_{th}
WF temperature (max), see §2.3	$T_{1,\text{max}}$	max(320 °C, T_{TD})
WF pressure (max), see §2.3	$P_{1,\text{max}}$	25 bar
net power output	$\dot{W}_{\text{ORC}}$	10 kW_{e}
condenser pressure (min)	$P_{6,\text{min}}$	0.3 bar
condenser temperature (min)	$T_{6,\text{min}}$	50 °C
cooling water temperature (in)	$T_{\text{H2O,in}}$	20 °C
Regenerator temperature diff. @ pinch point	$\Delta T_{\text{PP,REG}}$	10 °C
Degree of superheating (for subcritical cycles)	ΔT_{sh}	10 °C
Heat exchangers pressure losses	ΔP_{HX}	max(1.0 % P_{in}, 0.1 bar)
Turbine efficiency	$\eta_{\text{ts,TURB}}$	70 %
Pump hydraulic efficiency	$\eta_{\text{is,PUMP}}$	50 %
Mechanical transmission efficiency	$\eta_{\text{m,TRANSM}}$	92 %
Electric machine efficiency	$\eta_{\text{e,EM}}$	96 %

The first design constraint pertains to the delivered power $\dot{W}_{\text{ORC}}$ which is set to the value of interest of 10 kW_{e}. In order to achieve higher cycle efficiency, the condensing pressure P_6 has to be lowered with respect to that chosen for the nozzle TS (see §2.4), and sub-atmospheric values must be accepted. The minimum value of 0.3 bar has been selected following a trade-off analysis which considered the thermodynamic advantages (e.g., increased turbine work) and the techno-economical disadvantages (e.g., increased dimensions of the equipment due to the large volumetric flows) related to a decrease of P_6. Furthermore, as we explained in §3.6, proper means are needed to reduce another negative effect of this choice, i.e., those related with the intakes of ambient air into the set-up. Also the minimum condensing temperature T_6 is constrained, and a value of 50 °C is selected which can be guaranteed under all foreseen operating conditions (e.g., given the maximum temperature of the ambient air used for cooling). As for the nozzle TS, also in this case the performance of the heat exchangers, expressed by the pinch point temperature differences ΔT_{PP} within the same devices, have been given values taken from common practice in the ORC field. However, the $\Delta T_{\text{PP,REG}}$ has been lowered to 10 °C, with the aim of achieving better cycle efficiency. A turbine total-to-static efficiency (i.e. $\eta_{\text{ts,TURB}}$) of 70 % is assumed which, according to preliminary calculations performed on machines of this type, seems to be within practical reach [8]. All the remaining quantities in Table 2.4 have been given the same values considered for the nozzle TS (see Table 2.2). Notably, in the present case the losses due to the mechanical transmission and to the efficiency of the electric machines have been considered not only for the pump, but also for the turbine assembly, through the value of $\eta_{\text{m,TRANSM}}$ and $\eta_{\text{e,EM}}$.

Procedure

The design procedure for the turbine TS is based on a system-level optimization aimed at maximizing a single objective, i.e., the cycle thermal efficiency $\eta_{\text{th,ORC}}$. The considered optimization variables are the thermodynamic conditions at the turbine inlet, i.e., T_1 and P_1, and the condensing pressure P_6 (nomenclature referring to Fig. 2.1). For each of the WF's of interest (see Table 2.1), these quantities are varied within the ranges defined by the constraints collected in Table 2.4. Notably, depending on the WF characteristics, this allows to consider both subcritical and supercritical cycle arrangements. For the latter, a minimum degree of superheating [9] is specified, i.e. 10 °C , while for the former a minimum value of T_1 is estimated as a function of P_1 by following the same approach adopted for the

[9] The temperature increase with respect to the saturation value at the given pressure

nozzle TS (see §2.4). All the thermodynamic state points constituting the ORC can thus be calculated. This, in turn, allows to evaluate $\eta_{\text{th,ORC}}$.

Results

The results follow the analysis conducted by means of the in-house code *ORC-VPE 1.0*. An evolutionary optimization algorithm is used as the numerical method to solve the problem. For a more detailed description, the reader is referred to a recent work by Bahamonde and colleagues [5].

The analysis of the cycle calculation results shows that few candidate WF's allow to reach $\eta_{\text{th,ORC}}$ values around 20%, which is the target system performance. These WFs are siloxane MM, PFC's PP2 and PP90, and toluene. Notably, a value of $\eta_{\text{th,ORC}} \approx 20\%$ is very ambitious for such a small experimental system, since these performance levels are nowadays achieved by state-of-the-art ORC turbogenerators in the power range of hundreds of kW_e [10]. The detailed results concerning only the above mentioned fluids are shown in

Table 2.5: Results of the thermodynamic cycle calculation related to turbine-testing operation, limited to candidate WF's (see Table 2.1) allowing to reach a cycle net thermal efficiency of the order of 20%.

fluid	$\dot{Q}_{\text{in}}$ [kW_th]	$\dot{Q}_{\text{REG}}$ [kW_th]	$\dot{Q}_{\text{COND}}$ [kW_th]	$\dot{W}_{\text{PUMP}}$ [kW_e]	T_1 [°C]	P_1 [bar]	P_6 [bar]	T_6 [°C]	$\eta_{\text{th,ORC}}$ [–]	$\dot{m}_{\text{WF}}$ [kg/s]
MM	48.9	53.4	38.5	1.1	300	22.0	0.30	63	18.2	0.17
PP2	44.9	74.4	34.4	0.9	320	22.0	0.43	50	20.2	0.35
PP90	55.1	93.7	44.8	1.2	320	20.0	0.30	88	16	0.48
Toluene	47.7	21.6	36.9	0.6	320	25.0	0.30	73	19.7	0.09

Table 2.5, from which it can be concluded that:

- as expected, the thermodynamic optimization leads to cycles reaching the limiting values for both the $T_{\text{WF,max}}$ and the P_6 constraint (the only objective is the cycle efficiency); and
- the power input, mass flow rates, and HX's thermal loads are considerably lower than those resulting for the nozzle experiment (see Table 2.3).

2.6 Siloxane MM as the *design fluid*

By comparing the results pertaining to the design of the nozzle and of the turbine TS's, collected respectively in Table 2.3 and 2.5, it can be seen that different candidate WF's are expected to be suitable for both experiments. In order to proceed with the design of the ORCHID, it was decided to select one single fluid among all those reported in Table 2.3 and 2.5 for the preliminary design of the BoP, and in particular of the heat exchangers (*design fluid*). The design fluid is siloxane MM since:

- it requires for the nozzle experiment the largest input thermal power among the WF's considered at this stage and, in this sense, dimensioning the BoP with MM as the WF can be considered as a conservative choice based on the principle of dimensioning the equipment on the worst-case-scenario,
- it is already successfully employed in commercial ORC power systems,
- there are data about its thermal stability characteristics [38], and accurate thermodynamic models have been developed to predict its properties [14], and
- it is bulk-produced for the cosmetic industry, and its cost is thus comparatively low.

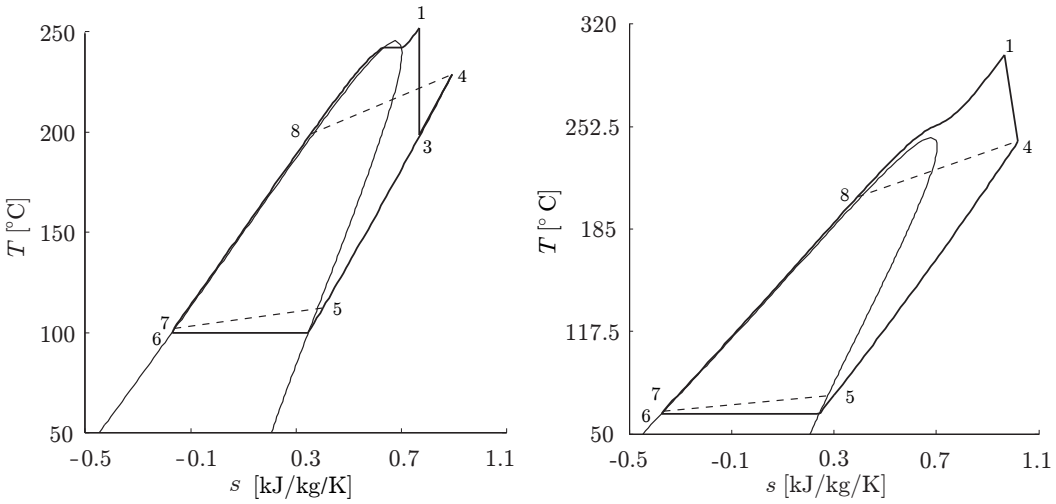

(a) (b)

Figure 2.6: $T - s$ diagram of Siloxane MM, showing the ORCHID thermodynamic cycles during nominal operation of the two TS's. a: nozzle TS in operation (see Table 2.6 for the state-points details), b: turbine TS in operation (see Table 2.7 for the state-points details).

Siloxane MM will therefore be the first WF to be tested in the ORCHID. However, the design of the BoP has to be verified also against the operating conditions required by all the other fluids (see Table 2.3 and 2.5), as detailed in the next section.

2.7 Nominal Operating Conditions

The complete details about the state-points constituting the ORCHID thermodynamic cycles are collected in the two summarizing tables which follow, i.e., Table 2.6 for the nozzle experiment, and Table 2.7 for the turbine experiment. Since siloxane MM is adopted as the design fluid, the data relative to this fluid are labeled *design* in the tables, while those pertaining to the other WF's, which have to be considered for *verification* purposes (i.e., those collected in tables 2.3 and 2.5), are labeled consequently. As it is explained in §3.3, Therminol 66 is the heat transfer fluid considered for use in the electric oil heater fluid loop, and the properties of this compound have been used to evaluate the quantities of state points 11 and 12.

2.8 Conclusions

This chapter presents the methodology developed for the design of the BoP of the ORCHID set-up, based on the analysis of the various processes forming the thermodynamic cycle. The aim of this analysis was to assess the potential of the proposed concept, i.e., a single BoP for continuous operation of either of two experiments as described in §2.1. The analysis was bounded by a number of general constraints of different nature, as detailed in 2.3. Several candidate working fluids (WF's) were considered, as explained in §2.2. The main results of the analysis are as follows:

1. As detailed in §2.4, a BoP is conceivable for the ORCHID set-up which allows to perform the envisaged fundamental studies in the NICFD field. The nozzle throat area is fixed to the value of 200 mm^2 and, under the assumptions collected in Table 2.2, only few WF's among those collected in Table 2.1 are compatible with the desired experimental conditions and, in particular, with a reduced pressure at the beginning

Table 2.6: Operating conditions for the nozzle TS thermodynamic cycle, see also Fig. 2.6. The data for the WF siloxane MM are those to be used to size all the BoP components, i.e. for design purposes. The data for the other WF's have to be considered for verification purposes.

	Quantity	Design	Verification			
		MM	MDM	PP2	PP90	D_4
Cycle general results	$\dot{m}_{\mathrm{WF}}$ [kg/s]	1.55	1.55	3.01	2.58	1.59
	$\dot{Q}_{\mathrm{in}}$ [$\mathrm{kW_{th}}$]	352.2	290.9	301.7	235.2	259.8
	$\dot{Q}_{\mathrm{COND}}$ [$\mathrm{kW_{th}}$]	359.8	297.5	309.1	240.2	265.4
	$\dot{Q}_{\mathrm{REG}}$ [$\mathrm{kW_{th}}$]	315.1	284	254.1	253.8	266.8
	$\dot{W}_{\mathrm{PUMP}}$ [$\mathrm{kW_e}$]	8.6	7.4	8.4	5.6	6.3
State-point 1	P_1 [bar]	18.4	15.6	22.7	17.6	14.7
PHX	T_1 [°C]	252	299	219	264	321
Outlet/	h_1 [kJ/kg]	355.9	419.8	137.1	204.2	413.0
Nozzle Inlet	$\dot{V}_1$ [l/min]	726	428	346	288	386
State-point *	P_* [bar]	12.4	11.3	16.4	12.7	10.6
Nozzle Throat	T_* [°C]	239	284	204	251	306
Conditions	h_* [kJ/kg]	349.5	416.8	135.3	202.8	410.4
	ρ_* [$\mathrm{kg/m^3}$]	68	100	254	243	112
	c_* [m/s]	113.6	77.5	59.1	53.0	71.0
	$\mathrm{A^*}$[$\mathrm{mm^2}$]	200	200	200	200	200
State-point 3	P_3 [bar]	2.1	2.1	2.1	2.1	2.1
Nozzle	T_3 [°C]	207	257	169	227	282
Outlet/	h_3 [kJ/kg]	311	391	117.0	190.0	389.8
Receiver	ρ_3 [$\mathrm{kg/m^3}$]	9	12.2	21.1	26.3	14.6
Inlet	U_3 [m/s]	299.9	239.9	200.5	168.6	215.2
	$\mathrm{A^*/A_3}$ [-]	0.348	0.377	0.282	0.344	0.394
	$\mathrm{M_3}$ [-]	2.0	1.9	2.0	1.9	1.8
State-point 4	P_4 [bar]	2.1	2.1	2.1	2.1	2.1
Receiver Outlet/	T_4 [°C]	230	271	189	240	295
Throttling Valve	h_4 [kJ/kg]	355.9	419.8	137.1	204.2	412.9
Inlet	$\dot{V}_4$ [l/min]	10,902	7,907	9,003	6,074	6,741
State-point 45	P_{45} [bar]	1.1	1.1	1.1	1.1	1.1
Throttling Valve	T_{45} [°C]	229	270	188	240	294
Outlet/	h_{45} [kJ/kg]	355.9	419.8	137.1	204.2	412.9
Regen. Hot Inlet	$\dot{V}_{45}$ [l/min]	21,260	15,580	17,559	11,917	13,310
State-point 5	P_5 [bar]	1.0	1.0	1.0	1.0	1.0
Regen.	T_5 [°C]	122	174	97	146	197
Hot Outlet/	h_5 [kJ/kg]	153.2	236.5	52.6	105.7	245.5
Condenser Inlet	$\dot{V}_5$ [l/min]	17,963	13,741	15,157	10,445	11,810
State-point 6	P_6 [bar]	1.0	1.0	1.0	1.0	1.0
Condenser Outlet/	T_6 [°C]	100	153	75	124	176
Pump Inlet	h_6 [kJ/kg]	-78.3	44.5	-50.1	12.6	78.9
	$\dot{V}_6$ [l/min]	130	135	102	90	123
State-point 7	P_7 [bar]	18.5	15.7	22.8	17.7	14.8
Pump Outlet/	T_7 [°C]	102	154	77	126	177
Regen.	h_7 [kJ/kg]	-73.4	48.8	-47.6	14.5	82.4
Cold Inlet	$\dot{V}_7$ [l/min]	129	134	101	89	122
State-point 8	P_8 [bar]	18.5	15.7	22.8	17.7	14.8
Regen. Cold	T_8 [°C]	192	237	157	208	261
Outlet/	h_8 [kJ/kg]	129.3	232.0	36.8	112.9	249.9
PHX Inlet	$\dot{V}_8$ [l/min]	165	168	126	113	153
State-point 9	T_9 [°C]	20	20	20	20	20
Air Cooler Delivery	$\dot{m}_{9,\mathrm{water}}$ [kg/s]	4.3	3.6	3.7	2.9	3.2
State-point 10	P_{10} [bar]	≈ 1.0	≈ 1.0	≈ 1.0	≈ 1.0	≈ 1.0
Air Cooler Return	T_{10} [°C]	40	40	40	40	40
State-point 11	T_{11} [°C]	277	324	244	289	345
Oil Heater Delivery	$\dot{V}_{11}$ [$\mathrm{m^3/h}$]	39.1	31.6	34.2	26.0	27.9
State-point 12	T_{12} [°C]	261	308	228	273	329
Oil Heater Return	$\dot{m}_{12,\mathrm{oil}}$ [kg/s]	9	6.9	8.1	5.9	6.0

Table 2.7: Operating conditions for the turbine TS. The data for the WF siloxane MM are those to be used to size all the BoP components, i.e. for design purposes. The data for the other WF's have to be considered for verification purposes.

	Quantity	Design	Verification			
		MM	MDM	PP2	PP90	Toluene
Cycle general results	$\dot{m}_{\mathrm{WF}}$ [kg/s]	0.17	0.26	0.35	0.48	0.09
	$\dot{Q}_{\mathrm{in}}$ [$\mathrm{kW_{th}}$]	48.9	61.4	44.9	55.1	47.7
	$\dot{Q}_{\mathrm{COND}}$ [$\mathrm{kW_{th}}$]	38.5	51.1	34.4	44.8	36.9
	$\dot{Q}_{\mathrm{REG}}$ [$\mathrm{kW_{th}}$]	53.4	78.0	74.4	93.7	21.6
	$\dot{W}_{\mathrm{PUMP}}$ [$\mathrm{kW_e}$]	1.1	1.1	0.9	1.2	0.6
State-point 1	P_1 [bar]	22	14	22	20	25
PHX	T_1 [°C]	300	320	320	320	320
Outlet/	h_1 [kJ/kg]	466.1	492.7	271.3	281.1	438.7
Nozzle Inlet	$\dot{V}_1$ [l/min]	89	148	110	99	86
State-point 4	P_4 [bar]	0.45	0.45	0.58	0.45	0.45
Receiver Outlet/	T_4 [°C]	249	284	282	287	233
Throttling Valve	h_4 [kJ/kg]	398.4	449.9	239.0	257.8	314.6
Inlet	$\dot{V}_4$ [l/min]	5,915	6,820	4,761	6,109	5,514
State-point 5	P_5 [bar]	0.35	0.35	0.48	0.35	0.35
Regen.	T_5 [°C]	77	126	63	102	87
Hot Outlet/	h_5 [kJ/kg]	79.6	155.0	26.2	64.4	77.2
Condenser Inlet	$\dot{V}_5$ [l/min]	5,029	6,184	3,403	5,167	5,010
State-point 6	P_6 [bar]	0.30	0.30	0.43	0.30	0.30
Condenser Outlet/	T_6 [°C]	63	112	50	88	73
Pump Inlet	h_6 [kJ/kg]	-150.5	-38.0	-71.7	-28.0	-328.1
	$\dot{V}_6$ [l/min]	13	22	11	16	7
State-point 7	P_7 [bar]	22.2	14.1	22.2	20.2	25.3
Pump Outlet/	T_7 [°C]	65	113	52	89	75
Regen.	h_7 [kJ/kg]	-144.8	-34.3	-69.3	-25.8	-322.1
Cold Inlet	$\dot{V}_7$ [l/min]	13	21	11	16	7
State-point 8	P_8 [bar]	22.2	14.1	22.2	20.2	25.3
Regen. Cold	T_8 [°C]	210	249	221	248	190
Outlet/	h_8 [kJ/kg]	174.0	260.6	143.5	167.5	-84.8
PHX Inlet	$\dot{V}_8$ [l/min]	19	30	49	27	8
State-point 9	T_9 [°C]	20	20	20	20	20
Air Cooler Delivery	$\dot{m}_{9,\mathrm{water}}$ [kg/s]	0.46	0.61	0.41	0.53	0.44
State-point 10	P_{10} [bar]	≈ 1	≈ 1	≈ 1	≈ 1	≈ 1
Air Cooler Return	T_{10} [°C]	40	40	40	40	40
State-point 11	T_{11} [°C]	325	345	345	345	345
Oil Heater Delivery	$\dot{V}_{11}$ [$\mathrm{m^3/hr}$]	5.3	6.6	4.8	5.9	5.1
State-point 12	T_{12} [°C]	309	329	329	329	329
Oil Heater Return	$\dot{m}_{12,\mathrm{oil}}$ [kg/s]	1.2	1.4	1.0	1.3	1.1

of the expansion $P_{1,\mathrm{R}} = 1.1$. These are siloxanes D_4 and MDM; and perfluorocarbons PP2, PP80 and PP90. Another WF of particular interest, i.e., siloxane MM, can be considered among the suitable compounds upon reducing the inlet pressure requirement to $P_{1,\mathrm{R}} = 0.95$. The corresponding results are listed in Table 2.3.

2. As detailed in §2.5, a BoP is conceivable for the ORCHID set-up which allows to perform the envisaged experiments on ORC turbines and systems in the power range of 10 $\mathrm{kW_e}$. Under the assumptions collected in Table 2.4, only few WF's among those collected in Table 2.1 are compatible with the desired experimental conditions and, in particular, with a cycle thermal efficiency of the order of 20 %. These are siloxane MM, perfluorocarbons PP2 and PP90, and toluene. The corresponding results are listed in Table 2.5.

3. Based on the calculated results, the set-up concept presented in §2.1 has been positively assessed. The layout and constraints are compatible with the possibility of performing all the experiments of interest with several WF's. However, the large variations of process variables among different experiments and WF's require special design solutions.

4. As detailed in §2.6, siloxane MM is chosen among the selected WF's as the *design fluid*, i.e., the WF on which the sizing of the BoP components is based, as described in the following chapters.

5. As detailed in §2.7, the nominal design operating conditions are collected in Table 2.6 for the nozzle experiment, and in Table 2.7 for the turbine experiment. As anticipated, the data pertaining to MM (indicated as *Design* in the tables) are used to size the BoP components. The data pertaining to the other WF's (indicated as *Verification* in the tables) are used to verify that the obtained BoP design still conforms to the requirements allowing to test all the WF's of interest. In general, and for all the WF's of interest, the nozzle experiments require a thermal input which is one order of magnitude larger than what is required by the turbine experiments. Consequently, the circulating WF mass flow rate and the thermal load of all the HX's are much larger in this case. On the contrary, the turbine experiments require more demanding HX's performance in terms of maximum WF temperature. As detailed in the next chapter, this has relevant implications.

Chapter 3

Requirements and Specifications for the BoP Hardware

This chapter summarizes the specifications of the BoP hardware, following the results of the previous chapter. The design of the nozzle and of the turbine test sections is not treated. The only preliminary specifications of the test sections affecting the BoP design described here are the length and width of the skid that accommodates them. The BoP can then be appropriately designed around them. Besides the design specifications for the main components of the BoP, technical solutions are proposed. These design solutions should be taken as options open for discussion with the company in charge of detailed design and construction of the ORCHID BoP, and need to be verified with the OEM's supplying all the components. For this reason open questions are also included in the treatment.

As a general requirement valid for all the components, the main construction material must be stainless steel. This not only includes primary hardware but also piping, valves, and instrumentation. The main reason is that the presence of metal oxides can enhance the thermal degradation reactions of the adopted WF's, see also §2.2. Moreover, pressure equipment of the set-up has to be designed with a safety margin of 2, namely considering for its sizing an operating pressure double the nominal value. If this is not possible or too complicated to be implemented, e.g., for high-temperature components such as the PHX, a safety margin of at least 1.6 shall be guaranteed. All set-up equipment pertaining to the working fluid circuit will be subjected to a water-pressure test prior to its acceptance.

3.1 APP Laboratory Location and Layout

The ORCHID facility will be located within the Aerospace Propulsion and Power (APP) Laboratory which is being constructed in the compressor hall of the Aerodynamic High Speed building (HSL) at Kluyverweg 2, Delft, 2629 HS. The space dedicated to the ORCHID is shown in Fig. 3.1, indicated as Zone A. It features a surface area of about 20 m^2, while the heater and cooling water loops will be located externally to the lab (Zone B and C, respectively). Several air coolers are already installed to serve the HSL (Zone D), and might be considered as a complementary source of cooling power for the ORCHID set-up. It is to be noted that another facility, called Combustion Lab. (Zone E), will operate alongside the ORCHID. It is a set-up which uses several potentially hazardous gases such as hydrogen, oxygen, and methane (supplied through low pressure lines from 50 liters standard cylinders located outside the HSL) for combustion tests. The potential risks induced by the combustion Lab., and how these should be kept into account while designing the ORCHID BoP, is left for investigation to the company performing the detailed design of the ORCHID.

Figure 3.2 provides a more detailed view of what is indicated as zone A in Fig. 3.1, i.e., the ORCHID set-up space, with the estimated dimensions of the main components and of the room required for optical measurements. All the ORCHID components, i.e., both

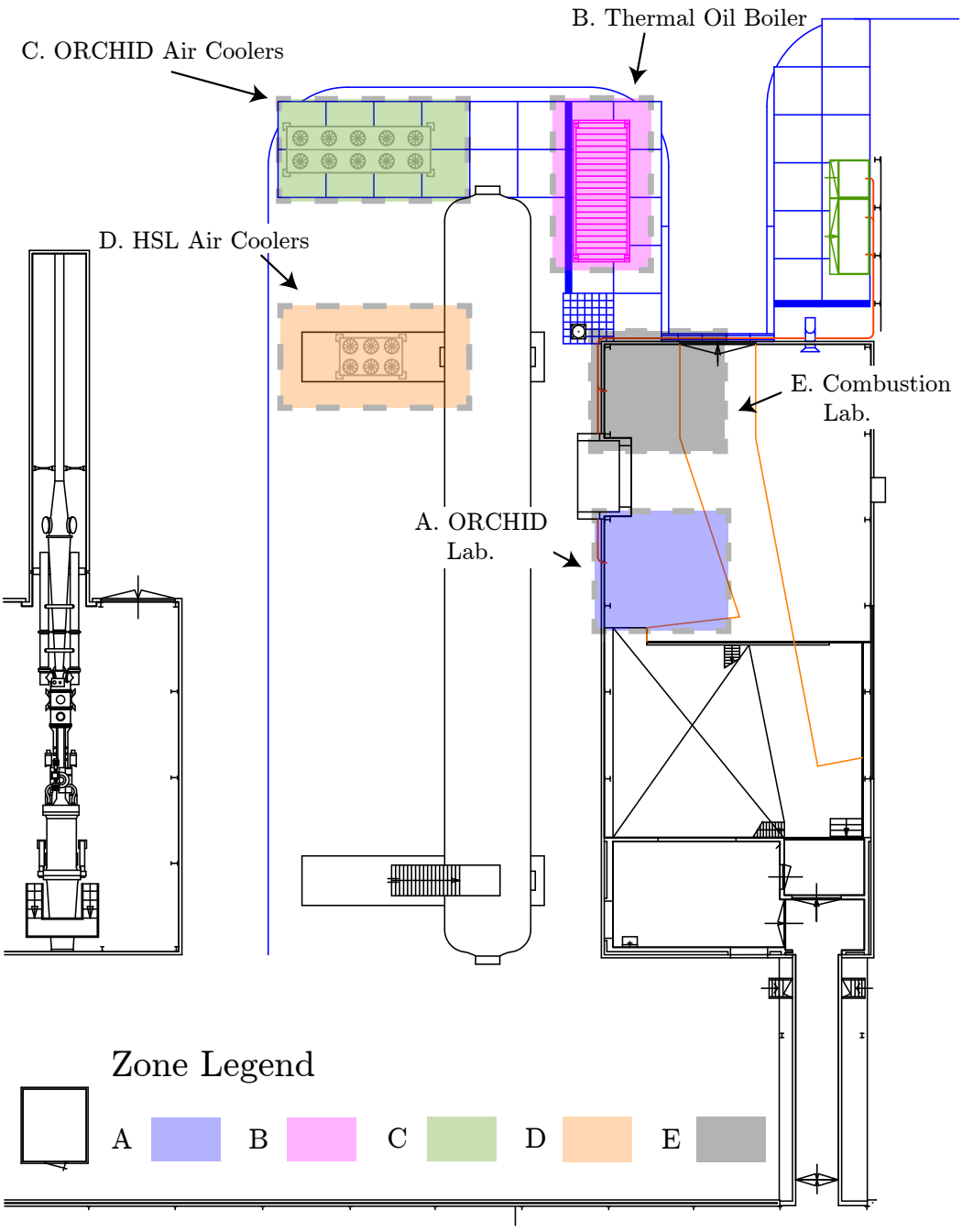

Figure 3.1: Schematic Layout of the High Speed Lab. showing the main zones. A: ORCHID Lab., B: Thermal Oil Boiler, C: ORCHID Air Coolers, D: HSL Air Coolers and E: Combustion Lab.

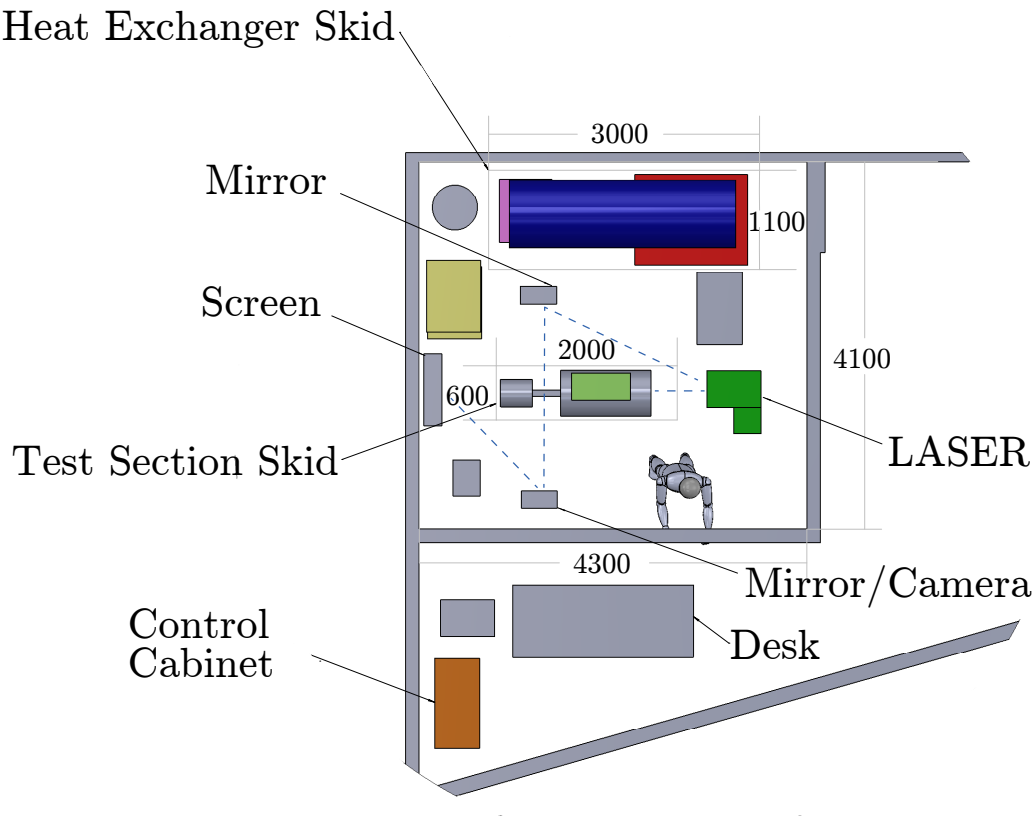

Figure 3.2: Detailed view of the space allocated for the ORCHID Lab. within the High Speed Lab., i.e., detailed view of what is indicated as zone A in Fig. 3.1. The main components of the optical measurement system are also shown, i.e., the LASER, mirrors, and screen, as well as the optical path (blue dashed line).

the BoP and TS's, must be placed in a *test room* isolating them from the rest of the HSL hall. The primary function of the room is to circumscribe the risk of fire and leakage of hot vapors[1] in a controlled enclosure with suitable ventilation and fire prevention systems. The main requirements of this test room are briefly outlined in the following list:

- The room should have a door, glass windows with metallic-net inserts and a lighting/electrical system;
- It must be equipped with a fire prevention system and fire proof ventilation;
- Because the ORCHID facility is heated permanently during the experimental session (i.e., for several days), ventilation is needed to maintain constant environmental conditions (≈ 25 °C);
- The estimated volume of the room is 60 m^3 thus the ventilation should provide ca. 1000 m^3/h;
- It should be equipped with an oxygen level sensor to check that no relevant leakage can pose a danger to the operator;

[1]Notably, these risks are relatively low because the fluids employed have low flammability and tend to condense when released into the environment.

- The bridge crane should be able to access the ORCHID area. A removable roof is thus needed;
- In case any working fluid from the ORCHID facility leaks, the flooring of the test room should prevent any outflow to the HSL hall;
- The room should be equipped with acoustic foam panels to attenuate noise generated during the experiments. Moreover, noisy components like the turbine shall have a dedicated noise insulation system; and
- Wiring of the facility shall be such as to allow remote control. Control panels and monitors of the control system will be installed outside the room as shown in Figure 3.2.

3.2 Test Section Positioning

A simplified layout of the ORCHID set-up is shown in Fig. 3.3, with the main components depicted as prisms. The area in which the TS's will be placed is worth particular attention: it must be possible to operate both the TS's independently. To this end, a stacked solution whereby the turbine is placed on top of the nozzle in a rack or skid could be a possibility. The BoP must thus have inlet and outlet ports at the interfaces with the TS's, and a by pass system to allows the operator to select which TS to use. The proposed location for the skid in which the TS's are stacked upon one another can be seen in both Fig. 3.2 and Fig. 3.3. The area occupied by the TS's skid must satisfy the following space and configuration requirements

- The two TS's should be mounted on a skid in a vertical configuration with the turbine stacked on top of the nozzle. The skid occupies a volume of approximately 2 x 0.6 x 1.8 m (length x width x height); and
- The arrangement of the BoP should allow for an easy access to the TS's, while preserving the space needed to perform the envisaged measurements. In particular, the optical measurement techniques require several pieces of equipment (such as, e.g., a LASER, a camera, and several mirrors) positioned around the TS's skid as shown in Fig. 3.2. Furthermore, the optical path between these components – depicted as a blue dashed line in the same figure – must not be obstructed. It is thus recommended that a minimum distance of 1 m surrounding the TS's skid is left free from any other infrastructure or component.

3.3 Thermal Oil Electric Heater

Among the various technical options for the transfer of energy as heat to the working fluid, the thermal oil electric heater has been selected, even if it is more expensive than other solutions such as, e.g., a gas burning heater. A thermal oil electric heater allows for an easy modulation of the thermal power, reducing the uncertainty in the system thermal input and consequently in the measurements. Moreover, industrial electric heaters employ thermal oils as the thermal fluid which provides several advantages with respect to steam. These advantages include

- the possibility to reach high temperatures (e.g., in excess of 300 °C) at atmospheric pressure, with lower operational risks and costs due to the lower pressure levels (no certified staff required);
- the possibility to avoid the pre-treatment of the thermal fluid, as is the case if water is adopted;
- the possibility to reduce the risk of corrosion or freezing of the thermal fluid; and

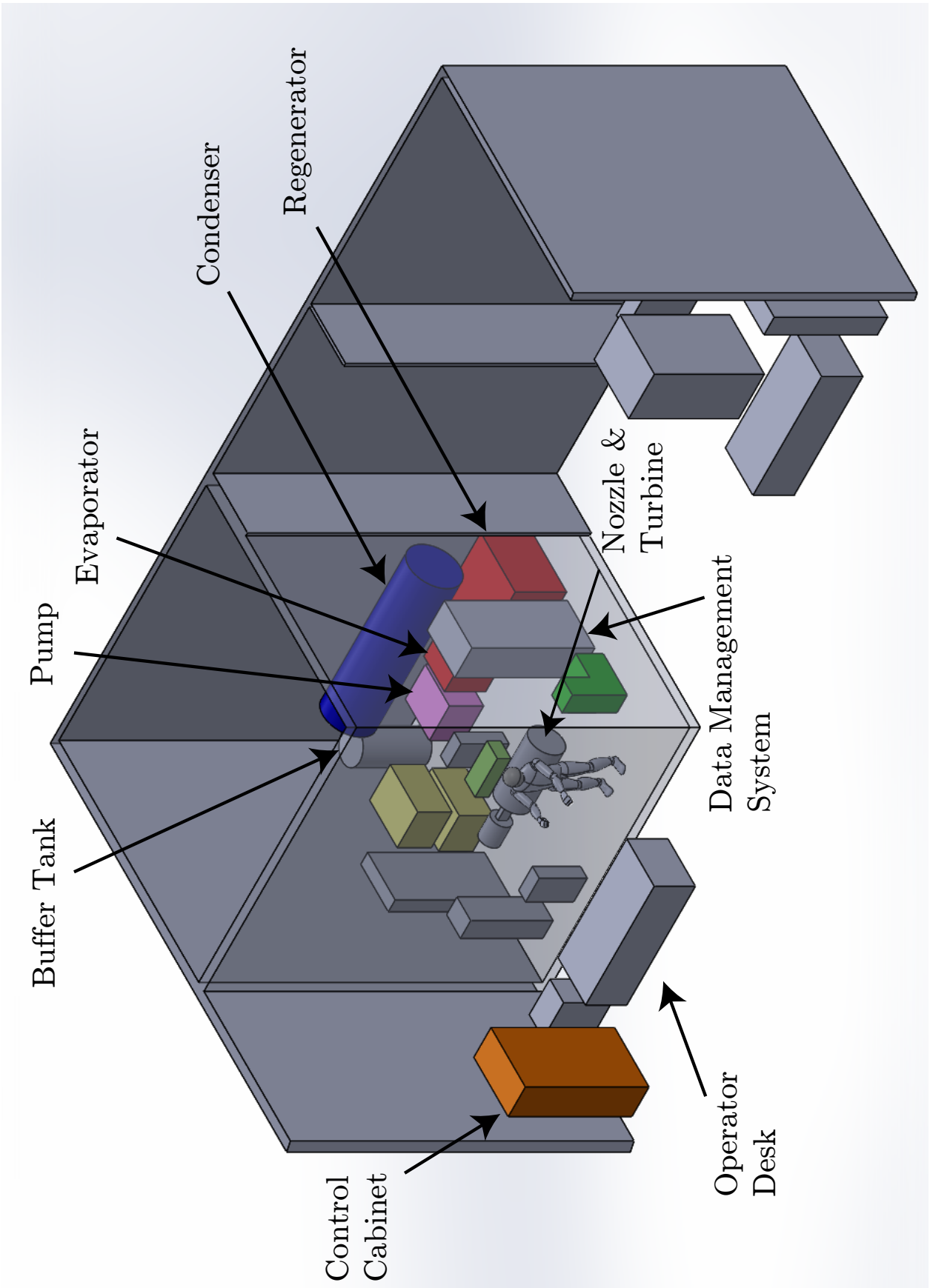

Figure 3.3: Schematic assembly of the ORCHID set-up, showing the test room and the proposed location of the workstation.

- lower maintenance costs.

The envisaged specifications for the thermal oil electric heater are summarized as follows.

- The capacity in terms of input electrical power must be as close as possible to the maximum available power of 400 kW_e (see also §2.3), and the maximum operating temperature for the thermal oil must be above 340 °C;
- It is preferable that the thermal fluid is low in toxicity. The thermal fluid considered hereafter in the document is Therminol 66;
- The heater shall be located outside the lab, i.e., in Zone B in Fig 3.1. Therefore, a containerized solution is arguably the best option, also to the end of ensuring the integrity of the heater in all environmental conditions (i.e., from −10 °C to 30 °C). The container must also be equipped with fire detection and extinction systems;
- The heater must be controlled remotely from Zone A (Fig 3.1). In particular, the electrical input must be easy to modulate in order to operate in part-load conditions;
- The oil boiler should be equipped with an expansion tank to prevent over-pressurizing the circuit and to handle the risks associated with oil leakage; and
- The feed and return oil lines which lie between Zone A and B (Fig. 3.1) must be insulated.

According to the knowledge gathered by discussing with heaters manufacturing companies, it appears that the most common operating mode for these components is to deliver a constant volumetric flow of HTF at a prescribed temperature. Furthermore, the temperature drop of the HTF between the heater inlet and outlet must be typically limited to values smaller than 20 °C. These characteristics have been considered in the calculations presented in the previous sections.

For the selection of the heater, it is thus fundamental to ensure that the heater can provide the needed HTF flow rate at the set temperature, for all operating conditions, i.e., those summarized in Tables 2.6 and 2.7. It is worth highlighting that these are specified at the entering ports of the primary heat exchanger and, as a consequence, all the thermal losses occurring within the heater (i.e., the heater thermal efficiency) and in the connecting pipes have also to be properly accounted for. As a preliminary estimation, all such losses should not account for more than 2.5% of the electrical power input or, in other words, the thermal power available on the oil side of the PHX should not be lower than 390 kW_{th} during nominal operation at maximum load.

3.4 Air Coolers

The cooling circuit of the facility is required to dissipate the maximum heat duty of the ORCHID, i.e., approximately 400 kW_{th}. The system consists of a cooling water loop that transports the thermal energy from the condenser to a bank of air coolers outside the building in Zone C (Fig. 3.1). A bank of air coolers, with a cooling power of $\approx 300 kW_{th}$ is already in use and is located in Zone D. These are used to cool the air delivered by the main HSL compressor before storing it. As the compression process takes place during the night, the HSL air coolers are not used during the day. For this reason, the possibility exists to exploit this existing hardware in order supply part of the cooling power needed by the ORCHID. This option shall be further discussed with the technicians of the HSL.

The envisaged specifications for the air coolers are summarized in the following list, and have been established in order to comply with the assumptions of the thermodynamic analysis presented in the previous chapter.

- The cooling capacity of the air coolers must be at least 400 kW_{th};

- The cooling water conditions at the condenser inlet should be: temperature ≈ 25 °C, and mass flow rate ≈ 4.0 kg/s. The expected increase of water temperature in the condenser is ≈ 20 °C;
- The air cooling system shall be located outside the lab, i.e., in Zone C (Fig 3.1), or be integrated with the existing air coolers, i.e., in Zone D;
- The air coolers (Zone C and/or D) should be remotely controlled from Zone A to regulate the delivery temperature of the water; and
- A mixture of glycol-water should be used to avoid freezing.

An open question which needs to be discussed is how to control the WF pressure in the condenser of the set-up. A possible option is to properly modulate the delivery temperature of the cooling water by controlling the rotational speed of the fans of the air coolers. It is probably not necessary to use a variable speed pump. This is to be checked with the company in charge of the detailed design of the set-up.

3.5 Primary Hardware

In this section the specifications regarding the main hardware components of the ORCHID BoP such as, e.g., the heat exchangers and the pump, are discussed.

Heat Exchangers

General guidelines have been derived for the design of these components. Companies that are partners in the ORCHID-related research projects and that will be contacted in relation to the procurement of the heat exchangers are: Bosch, Dana-Spicer, Nefit, Eastman Therminol. The heat duty of the heat exchangers (HX's) varies significantly depending on the test section in operation and the considered WF, as detailed in §2.7. This poses several design challenges, in particular regarding the sizing of the high-temperature HX's, i.e., the PHX and the regenerator.

Considering the nominal thermal load required at the PHX, for instance, this is typically one order of magnitude larger for the nozzle experiments than is for the turbine experiments. After a preliminary analysis, a viable solution to enhance the flexibility of the set-up in this sense is deemed that of adopting a configuration with several HX's in parallel. Instead of attempting to design a single HX able to cope with all the envisaged operating conditions, the required thermal load is split over a number of smaller HX's arranged in parallel. In this way, the number of HX's in operation can be easily controlled by excluding some of them from the circuit, in order to match the required thermal load while allowing to fine tuning the thermodynamic conditions at the HX's outlet. Several advantages are predicted, related to the possibility of operating the HX'sclose to their nominal operating point. This is expected to reduce the risk of significant drops of the heat transfer performance due to flow maldistribution, and thus the insurgence of hot-spots within the HX.

Furthermore, there are several particular issues which have to be accurately considered such as, in particular, the need of (i) allowing for the WF heating process at both supercritical and sub-critical pressure, and (ii) minimizing the surface area occupied by the set-up. A preliminary technology evaluation led to consider plate heat exchangers as the most promising solution for the high-temperature HX's of the ORCHID BoP, i.e., the PHX and the regenerator.

The preliminary sizing of these plate HX's can be performed by considering the operating condition for the turbine test section as the design point, while the number of units in parallel can be defined by matching the nozzle operating conditions. This approach is motivated also by the fact that, as discussed in §2.8 (see in particular point 5), the operating conditions for turbine testing are the most demanding, i.e., the temperature differences which must be established within the HX's are lower than what is needed for the nozzle

experiments.

The design of condenser, on the contrary, can be performed based on the larger thermal load requirement, i.e., that specified by the nozzle experiments. The compatibility of the obtained results with the operating conditions required for turbine testing is then checked a posteriori. A shell and tube heat exchanger seems more suitable to handle the sub-atmospheric conditions necessary for the turbine experiments, in particular regarding the venting of non-condensible gases during operation or before start-up. In order to reduce pressure drops, the condensing vapor flows in the shell, while the cooling water in the tubes.

The operating conditions for the design of the ORCHID HX's are provided in Table 3.1. As detailed in §3.3, the thermal oil Therminol 66 is assumed as the fluid adopted in the electric oil heater, while water is adopted in the cooling circuit. The design thermodynamic conditions of the considered fluid, i.e. siloxane MM (see §2.6), are collected in Table 2.6 for the nozzle experiment, and in Table 2.7 for the turbine experiment, and are added to Table 3.1 for the sake of clarity.

Table 3.1: Design input for the primary heat exchanger (PHX), the regenerator (REG) and the condenser (COND). The considered HTF is Therminol 66.

	Nozzle experiment						Turbine experiment					
	PHX		REG		COND		PHX		REG		COND	
Side	Hot	Cold	Hot	Cold	Hot	Cold	Hot	Cold	Hot	Cold	Hot	Cold
Phase	L	LV	V	L	VL	L	L	LV	V	L	VL	L
Fluid	HTF	MM				Water	HTF	MM				Water
$\dot{m}$ [kg/s]	9	1.55				4.3	1.2	0.17				0.46
$\dot{Q}$ [kW_{th}]	352		315		360		49		53		39	
T_{in} [°C]	277	192	229	102	122	20	325	210	249	65	77	20
T_{out} [°C]	261	252	122	192	100	40	309	300	77	210	63	40
P_{in} [bar]	≈ 1	18.4	1.1	18.5	1	≈ 1	≈ 1	22.2	0.45	22.2	0.3	≈ 1
$\dot{V}_{in}$ [l/s]	10.9	2.8	354.3	2.2	299.4	4.3	1.47	0.32	98.6	0.22	83.8	0.46

Some additional design specifications and requirements for the HX's are

1. The design of the HX's should be checked against the operating conditions for the different WF's (see §2.8).
2. Also the dynamic performance of the HX's must be carefully evaluated, both during nominal operation and start-up/shut-down procedures.
3. All the HX's should be stacked in a skid mounted configuration to make the entire set-up more compact.
4. With reference to zone A in Fig. 3.1, the HX skid should be located along the wall of the lab,
5. It should be possible to easily remove components of the HX's from the skid for maintenance purposes,
6. A venting system is required in the condenser to achieve and maintain sub-atmospheric pressure levels,
7. If a configuration with multiple HX's is adopted for the PHX and the regenerator, each HX should be equipped with a check valve to exclude it from the circuit and be instrumented with temperature and pressure measurement devices, and
8. All the HX's should be insulated to minimize heat losses in the system and to guarantee a safe operating environment.

Moreover, there are some technical questions pertaining the selection of HX's which have not been addressed yet and are thus left for further discussion with the company in charge of the detailed design/construction of the set-up. These are:

1. is there a possibility to clean the heat exchangers?
2. what is the allowable rate of change of heat load in order to avoid damaging the plate heat exchangers during start-up and shut-down procedures?
3. is the adoption of a configuration with multiple HX's in parallel advantageous from the economic and practical points of view?

System charge tank

A system tank after the condenser is needed to decouple the maximum and minimum pressures of the circuit by accommodating fluid density variation during operation. It is used also as a charging point of the circuit and as a storage tank when the facility is not in operation. The charge tank is required to

1. be sized to accommodate fluid density variation in all operating range of the set-up without the need of liquid level control; and
2. be insulated.

ORCHID Feed Pump

The feed pump should modulate the flow in the circuit in a wide operational range. With reference to Table 3.1 and 3.2, the volumetric flow at the pump inlet for the nozzle test section varies between 88-130 l/min depending on the working fluid, while for turbine testing the flow reaches a maximum value of 18 l/min in case of MDM. Whereas the differences between the two TS's in terms of pressure head required of the pump are limited, being the maximum pressure of the thermodynamic cycle in the range of 15 to 25 bar. These specifications fall within the operational range of volumetric pumps. In addition, the start-up of the facility is expected to require additional pumping power for reasons associated to stabilizing the supersonic flow and overcoming viscous effects in the nozzle and test section channel. The increase in pressure can be easily managed with a volumetric pump but may require an over sizing of the electric motor. Despite the high flexibility of these pumps in terms of mass flow rate control, it seems difficult to find a unique speed-controlled pump that can cover all the operational range required by two TS's. To comply with these requirements two design solutions have been considered, i.e.,

1. multiple pumps in parallel; or
2. a single variable speed pump with a bypass circuit.

The solution with the bypass seems more promising due to reasons associated with costs. Additionally the bypass circuit allows a smoother start-up to avoid over-pressurising the heat exchangers. Regardless of the chosen solution, a damper is required to smooth out flow fluctuations generated by the volumetric pump. The optimal position for the damper is probably downstream of the bypass circuit. The system pump must fulfill several requirements, i.e., it must be:

1. capable of a wide operational range (operating conditions that should be considered for the design are provided in Table 3.1);
2. equipped with a damper. Flow fluctuations should be limited to 0.5-1% of the nominal volumetric flow rate of the pump;

3. such that the required NPSH at the inlet is lower than 1-2 m since the current cycle configuration of the facility does not allow for an active control of the sub-cooling of the working fluid in the condenser (This issue can be possibly overcome by installing an additional heat exchanger downstream of the system tank); and

4. able to avoid contamination of the working fluid with the lubricant (if any).

Table 3.2: Design inputs of the System Pump (with siloxane MM as the working fluid)

	Nozzle	Turbine
$\dot{V}_{\text{in}}$ l/min	130	11
$\dot{W}_{\text{PUMP}}$ [kW$_e$]	7.6	0.9
T_{in} °C	100	63
P_{in} [bar]	1.0	0.3
P_{out} [bar]	18.5	22.2

Throttling Valve

This valve is located after the receiver of the nozzle test section, (after Station 4 of Figure 2.1). The aim of the valve is to decouple the pressure of the outlet of the nozzle and the pressure of the fluid as well as to vary the expansion ratio in the nozzle. The valve should:

1. be fast acting;

2. be designed for safe operation; and

3. feature a nominal pressure drop across it of 1 bar.

It is not yet known which valve flow characteristic (linear or equal percentage) is more suitable for operation.

3.6 Auxiliary Systems

A number of auxiliary systems are needed to ensure regular operation of the ORCHID facility. Among these, particularly important are the vacuum system and the Particle Image Velocimetry (PIV) circuit, which are described in the following.

Vacuum System

As discussed in §2.2, the adopted WF's tend to degrade at high temperature, and the presence of oxygen strongly enhances the involved reactions accelerating the WF decomposition. It is thus very important that

- the system is designed to be leak-tight, particularly regarding air intakes in sections that might be operated at sub-atmospheric pressure (e.g., during start-up). The fact that such sections can concurrently be heated up to high temperatures must also be considered;

- an inert-pressurization system must be designed, which allows to fill the set-up (or parts of it) with inert gases such as, e.g., nitrogen and helium. This serves at least two important purposes. Firstly, pressurizing with an inert gas at super-atmospheric pressures avoids air-intakes, and prolongs the fluids operative life. Secondly, pressurization with helium allows locating leakage with specialized equipment available in the lab. Given the required low pressure levels, and according to previous experience, the pressurization system can fruitfully exploit the same access points designed for the vacuum system (see next point), in order to reduce cost and complexity;

- a vacuum system is needed, which allows to extract all the non-condensible gases from the setup (or parts of it). A series of access points (or Vacuum Ports, VP) should be inserted in the most critical points of the setup such as, e.g., close to the most bulky components, i.e., the heat exchangers. Each VP should be equipped with an actuated valve. This would allow to implement automatic vacuum procedures, for instance during plant start-up, minimizing the risks related to operators' errors. All the VP's are connected to a single vacuum pump. According to previous experience, an absolute vacuum level in the system of the order of 1 mbar can be considered satisfactory. The VP could simply be vacuum connections welded to the BoP piping (open for discussion).

A preliminary arrangement of the VP's within the ORCHID facility layout is shown in Fig. 2.1.

PIV Circuit

In order to perform optical flow measurements based on the Particle Imaging Velocimetry (PIV) technique, the working fluid circulating in the system must be inseminated with particles acting as tracers. The envisaged tracers for the ORCHID experiments are titanium oxide particles with diameter between 50 μm and 150 μm. The amount of needed circulating particles is expected to be in the range of few grams per kg of circulating WF. The PIV circuit is the system of devices designed to inject and extract particles from the system, and the BoP needs to accommodate it.

The particles insertion needs to be performed during normal operation, i.e. with the running setup, in order to fine-tune the amount of circulating seeding. For this reason, a specially conceived device has to be designed to be connected to a flanged pipe welded in vertical position just downstream the liquid separator. This process connection is indicated as PIV Access Point (i.e., PIV-AP) in Fig. 2.1.
The particles extraction is performed before the facility shut-down by diverting the flow through the filtering branch, just downstream the pump bypass system. This process connection is indicated as PIV Filtering (i.e, PIV-F) in Fig. 2.1.

Chapter 4

Requirements and Specifications for the DAQ and Control Systems

4.1 Control System

The objectives of the control system are:

1. To guarantee the required operating conditions at the inlet and outlet of the TS's. The process variables which have to be tightly controlled in order to assure the reliability and success of the experiments are the temperature and pressure of the vapor in the settling chamber (or in the plenum before the two TS's) and the backpressure of the nozzle and the turbine. However, since a volumetric pump is most likely selected, a better controlled variable is the volumetric flow delivered by the pump rather than the TS's inlet pressure. Possible control loops are described in §4.2;

2. to manage the start-up (or shut-down) of the set-up by performing an appropriate sequence of procedures until the required operating conditions are reached. The start-up process should be fully automated due to the long time which may be needed and for safety reasons. A qualitative description of the main steps of the envisaged start-up procedure is illustrated in §4.3;

3. to minimize process disturbance effect on measurements (process disturbance rejection). Low frequency disturbances acting on the system are the variation over time of environmental conditions and of set-up heat losses as well as accumulation of incondensable gases in the condenser. High frequency noise in the process parameters is caused by mass flow fluctuations due to the intrinsically periodic operation of the volumetric pump of the system and fluid dynamic instabilities induced by the experiments in the nozzle TS. Despite process noise in the measurements can be minimized by averaging over time the acquired data thanks to the closed loop configuration of the set-up, for the success of the experiments it is desirable that the controller is able to maintain deviations from set point of main process variables within the following indicative ranges:

   - Fluid temperature at the inlet of TS's: $\pm$ 1 °C;
   - Pressure at the inlet of TS's in the range $\pm$ 0.2 bar
   - Back pressure (outlet pressure) of TS's in the range $\pm$ 0.02 bar.

   These ranges were determined so as to ensure that fluctuations of the main process variables of the nozzle experiment, namely the working fluid mass flow rate and the Mach number along the nozzle, are kept respectively within $\pm$ 2% and $\pm$ 0.5% of their target values. The resulting uncertainty level of the measurements is deemed adequate for the purposes of the experiments. A control system able to meet the

strict requirements needed for the nozzle TS might be suited also for the turbine TS, because the process variables to be measured in this case are much less sensitive to the set-up operating conditions.

4. To ensure operational safety and to protect the set-up equipment. The control system should comply with the ramp rates[1] compatible with the different component of the set-up. It should perform a safety shut-down of the system if a malfunction situation is detected (e.g. overpressure in the circuit, fire detection, ect.) and signal the anomaly to operators. The set-up operation can be also interrupted by the operators in case they recognize an emergency situation, for instance with an emergency stop button outside the laboratory.

The programming of the control system using a high-level graphical language (e.g. LabView) is highly recommended. This allows an easier modification of the control loops in case of future adaptations of the set-up as well as a simpler implementation by the P&P staff of data reconciliation and gross error detection algorithms for online monitoring of sensors accuracy.

4.2 Control Loop

This section describes a possible configuration for the control system, consisting of the following main control loops in parallel (see Figure 4.1).

1. **The first control loop** regulates the mass flow rate of the working fluid in the circuit and indirectly therefore the pressure at the inlet of the TSs. Given the temperature at the outlet of the PHX, the pressure is set by the flow characteristic of the nozzle or of the turbine. The manipulated variables are the rotational speed of the volumetric pump and the position of the actuator of the pump by-pass valve when the decrease of pump speed is not sufficient to reach the low mass flow rate required for turbine testing or is too inefficient.

2. **The second control loop** aims at regulating the working fluid temperature at the PHX outlet. The set-point of this temperature depends on the desired pressure at TS inlet in order to avoid fluid condensation during the expansion in the turbine or in the nozzle. In case of subcritical operation, the superheating is 5-10 °C. The manipulated variables are the set-points of the mass flow rate and delivery temperature of the thermal oil, which are managed by the controller of the electric heater.

3. **The third control loop** shall stabilize the condensing pressure of the system by regulating the rotational speed of the fans of the air coolers.

4. **The fourth control loop** adjusts the expansion ratio of the nozzle by varying the pressure drop in the throttling valve downstream of the nozzle receiver. The aim of this controller is to provide fast regulation of the expansion process and to reject pressure disturbances at the TS outlet. This is not achievable with the control loop that regulates the condensing temperature of the working fluid, due to the relatively high thermal inertia of the condenser and the cooling water circuit.

4.3 Start-Up

The main steps of the cold start-up procedure of the ORCHID are qualitatively described. Cold start-up means that the fluid that resides in the ORCHID circuit is at room temperature. The definition of this procedure is at the basis of the detailed design of the set-up because it allows to determine the auxiliary components of the facility, such as check valves,

[1] the rate at which the thermal load of a component can be increased or decreased

AC: Air Coolers
BD: Burst Disk
BPV: Buoyant Plug Valve
BT: Buffer Tank
CHX: Condenser Heat Exchanger
CV: Check Valve
DT: Dump Tank
D1...n: Drain Valves
FDP: Flow Damper
LS: Liquid Separator
NCV: Nozzle Control Valve
P: Pump
PB: Pump Bypass
PHX: Primary Heat Exchanger
PIV-AP: PIV- Access Point
PIV-F: PIV-Filter
RV: Relief Valve
RHX: Regenerator Heat Exchanger
SC: Settling Chamber
TOH: Thermal Oil Heater
TSC: Test Section Channel
TB: Turbine Bypass
TMV: Turbine Main Valve
VP : Vacuum Port
VV1...n :Vacuum Pump Circuit Valves
V1...n: Ball Valves

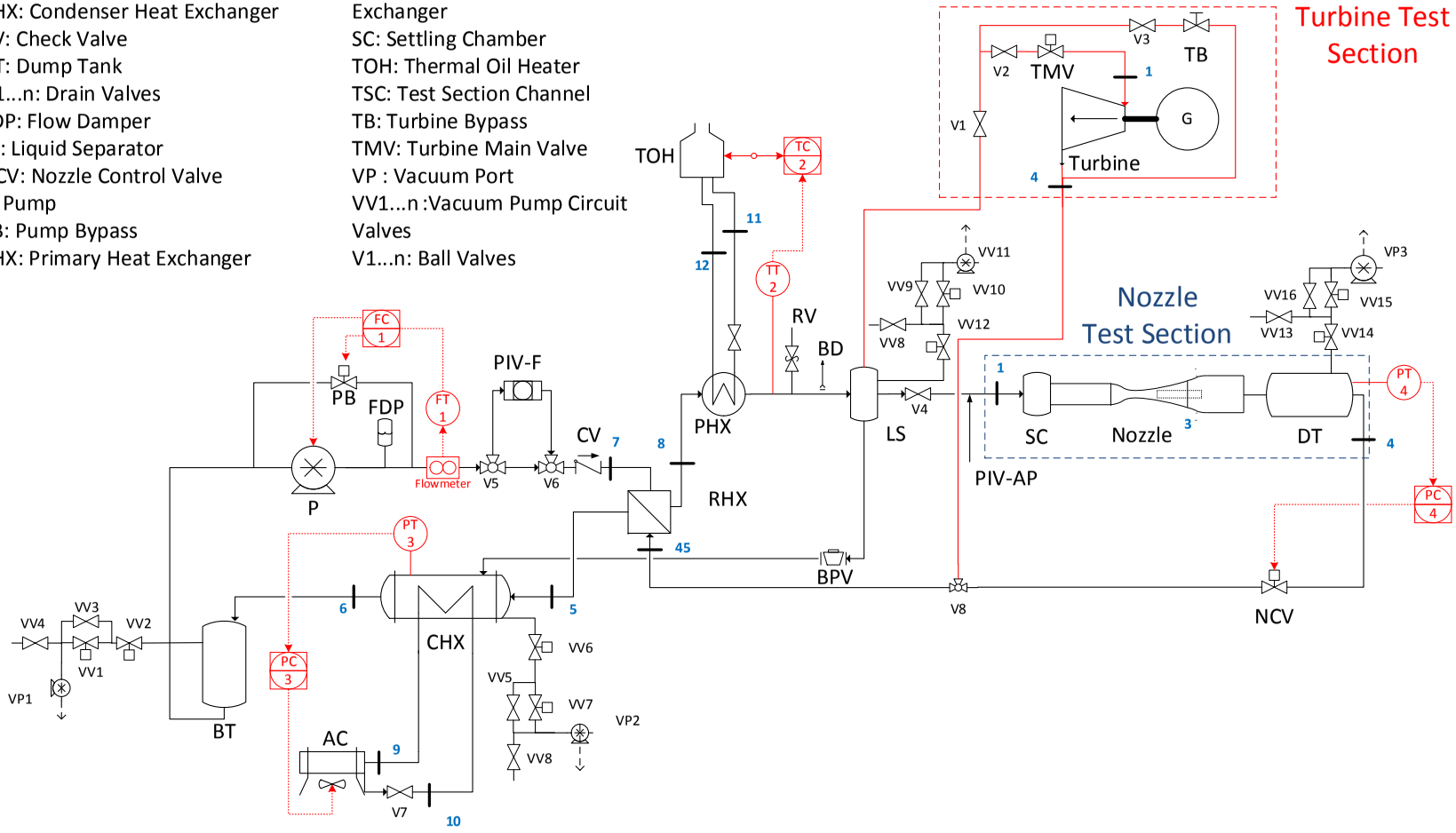

Figure 4.1: Detailed process flow diagram of the ORCHID facility including the main control loops of the control system (in red). The symbols adopted to represent the latter are the standardized symbols for P&I diagrams

by-pass loops, the liquid separator tank (see PFD in 2.1), etc. For this reason, the start-up sequence reported in the following for the nozzle TS [2] should be intended as a preliminary attempt aiming at establishing the specifications for the development of the Process and Instrumentation Diagram (P&ID) of the plant. The system shut-down is instead expected to be less relevant in this regard, because the process constraints involved in such operation (maximum time, allowable rates of load changes, etc.) are not so stringent as those of start-up. The shut-down procedure will be thus analysed when the P&I diagram of the ORCHID is defined with a higher degree of detail.
The start-up procedure consists of the following steps:

1. At cold conditions, assuming MM as working fluid, the condenser pressure should be between 40-70 mbar. If this is not the case, the vacuum pump is activated unill the pressure reaches the set value;

2. The valves at the inlet of the regenerator and TS shall be closed, while the throttling valve downstream of the nozzle and the by-pass valve of the pump are opened;

3. Cooling water circuit must be activated before any other operation;

4. The electric heater is started up and preheated;

5. The working fluid feed pump can now be put into operation, maintaining the by-pass valve fully open and the check valves on the regenerator admission closed;

6. The valve at the regenerator inlet is smoothly opened and the opening of the by-pass valve and the rotational speed of the pump are modulated in order to achieve the desired mass flow rate in the circuit. The value of the initial set-point for the working fluid mass flow rate depends on the allowable rate of change of the heat load in the PHX and the capacity of the liquid separator [3];

7. The thermal oil is sent to the PHX to heat up the working fluid. The oil temperature and mass flow rate are progressively increased in compliance with the allowable ramp rates for the heat exchanger;

8. The valve at the TS inlet is opened and dry vapor starts to circulate and warm-up the TS and the regenerator;

9. The control loop for condensing pressure is activated;

10. The working fluid and thermal oil mass flow rate are gradually increased until the nominal operating conditions required for the experiments are achieved. In order to prevent considerable fluid condensation in the TS, the load ramp should be such that highly superheated vapor is obtained at the PHX outlet;

11. Finally the desired backpressure of the nozzle is set by regulating the throttling valve downstream of the nozzle receiver.

[2] Turbine start-up has not been analyzed yet, since the design of this test section is at an initial stage.

[3] The liquid separator could be quite expensive due to the high temperature and pressures at which it operates. An alternative consists in realizing a by-pass circuit to conduct the working fluid to the set-up condenser till dry vapor condition at the PHX outlet are achieved. This can be accomplished quite quickly by a proper modulation of the mass flow rate pumped in the circuit. In such a case a sight glass should be placed on the by-pass pipe. When at a visual inspection the vapor stream appears dry, the by-pass valve is closed and the working fluid can start to flow in the TS. The drawback of this solution is that the start-up procedure cannot be fully automated.

4.4 Measurement Instrumentation

The set-up should be equipped with two decoupled measurement systems, one for the actual testing and one for monitoring and control purposes. This report deals only with monitoring and control instrumentation, whose components – the instruments to measure working fluid pressures, temperatures, and flow rates – equip the BoP. The preliminary configuration of these instruments is shown in Fig. 4.2, while Table 4.1 gives a brief description of the measurements to be performed at each station.

As a general consideration, the objective is to measure T and P of the fluid at all component interfaces, particularly at the inlet/outlet of the heat exchangers. No particular dynamic performance (i.e. high frequency response) is required. Considerations open for discussion are:

- Regarding the availability of high temperature pressure transducers note that for $T_{\max} > 250$ °C there are few manufacturers (MPI and Holykell); if the temperature is reduced to $T_{\max} < 250$ °C there are many more and also well known manufacturers (Swagelok, Kulite, Honeywell, Wika and Esi-tec)
- For the measuring stations corresponding to inlet/outlet of the heat exchangers, the sensors must be as close as possible to the heat exchangers themselves.
- The measuring stations must be easily reachable and sufficient room must exist to perform basic operations around the sensors.
- The pressure measurements are known to be particularly difficult in the presence of vapor in conditions close to saturation, since it is likely to have the formation of condensate in the lines/pipes bringing the pressure information to the sensor, which can severely alter the measurement. Several options exist to accurately perform these measurements, i.e.,
  - all the pressure sensors can be flush mounted. The main drawbacks are related to the need of having high$-T$ pressure transducers (expensive and inaccurate, drifting in time).
  - a purging system can be designed to inject a stream of inert gas in the transducers lines with the aim of emptying them from the condensate. Such non condensible gases can thus be extracted in the condenser. Heating up the lines is also an option. This solutions, which has already been tested in-house, allows to utilize more accurate (specially over time) and less expensive sensors, but obviously complicates the system.
  - an intermediate fluid (e.g., a thermal oil) can be used to route the pressure signal from the high$-T$ measurement station to the sensor. This is presently our preferred choice, and the company Wika manufactures these measuring devices.
- It is desirable that the P measurements allow to determine the thermodynamic state of the fluid or, in other words, that these are total quantities. A check is thus required regarding the flow velocities that are reached in the different stations, to confirm that the kinetic pressure is negligible. This might influence the determination of the piping diameters.
- In our experience, calibrating the instruments by sending them to a calibration center is a troublesome procedure, very expensive and time consuming, and it can negatively affect the availability of the rest of the setup (e.g., if this is leak-tight before calibration, a long time is required before this condition is established again after remounting the instruments). Furthermore, in case of high temperature P measurements, such a calibration never resembles the real sensor operating conditions. It could therefore make sense to provide each measuring station with an additional port (with a valve),

Table 4.1: Measurement stations description and instruments requirements, considering MM as the working fluid and the nozzle experiment only (process data from Table 2.6).

Pos.*	Measurement description & Instrument requirements	Estimated Accuracy
S1	T and P in low speed vapor. $P_{MM} = 21.3$ bar, $T_{MM} = 254$ °C. Strong need of avoiding condensation-related problems.	±0.1 bar. ±1 °C.
S4	T and P in low speed vapor. $P_{MM} = 2.1$ bar, $T_{MM} = 219$ °C. Mild need of avoiding condensation-related problems.	±50 mbar. ±1 °C.
S45	T and P in low speed vapor. $P_{MM} = 1.1$ bar, $T_{MM} = 218$ °C. Mild need of avoiding condensation-related problems.	±50 mbar. ±1 °C.
S5	T and P in low speed vapor. $P_{MM} = 1$ bar, $T_{MM} = 122$ °C. Strong need of avoiding condensation-related problems.	±10 mbar. ±1 °C.
S6	T and P in low speed liquid. $P_{MM} = 1$ bar, $T_{MM} = 100$ °C.	±10 mbar. ±1 °C.
S7	T, P, and flow rate in low speed liquid. $P_{MM} = 21.4$ bar, $T_{MM} = 102$ °C, $\dot{m}_{MM} = 125$ l/min = 7500 l/h ≈ 5500 kg/h. Note that certain flow meters (e.g., those based on Coriolis forces detection) provides also accurate measurements for density	±25 mbar. 1 °C. ±70 kg/h.
S8	T and P in low speed liquid. $P_{MM} = 21.4$ bar, $T_{MM} = 184$ °C.	±25 mbar. ±1 °C.
S9	T and P in low speed air. $P_{air} = 1.5$ bar, $T_{air} = 20$ °C.	±25 mbar. ±1 °C.
S10	T, P and flow rate in low speed air. $P_{air} = 1$ bar, $T_{air} = 40$ °C, $\dot{m}_{air} = 125$ kg/s.	±16 mbar. ±1 °C. ±3 kg/s.
S11	T in low speed HTF (e.g., thermal oil Therminol 66). It is assumed that a flow rate measurement (needed) is made available by the thermal oil heater assembly. $T_{HTF} = 380$ °C	±1 °C.
S12	T in low speed HTF (e.g., thermal oil Therminol 66). $T_{HTF} = 380$ °C	±1 °C.

* Position of the measuring station referring to the layout in Fig. 4.2

which can be used to calibrate the sensors on-line by subsequently connecting a reference instrument to each port while the setup is running in design conditions. This can be defined as an *in-situ* calibration.

AC: Air Coolers
BD: Burst Disk
BPV: Buoyant Plug Valve
BT: Buffer Tank
CHX: Condenser Heat Exchanger
CV: Check Valve
DT: Dump Tank
D1...n: Drain Valves
FDP: Flow Damper
LS: Liquid Separator
NCV: Nozzle Control Valve
P: Pump
PB: Pump Bypass
PHX: Primary Heat Exchanger
PIV-AP: PIV- Access Point
PIV-F: PIV-Filter
RV: Relief Valve
RHX: Regenerator Heat Exchanger
SC: Settling Chamber
TOH: Thermal Oil Heater
TSC: Test Section Channel
TB: Turbine Bypass
TMV: Turbine Main Valve
VP : Vacuum Port
VV1...n :Vacuum Pump Circuit Valves
V1...n: Ball Valves

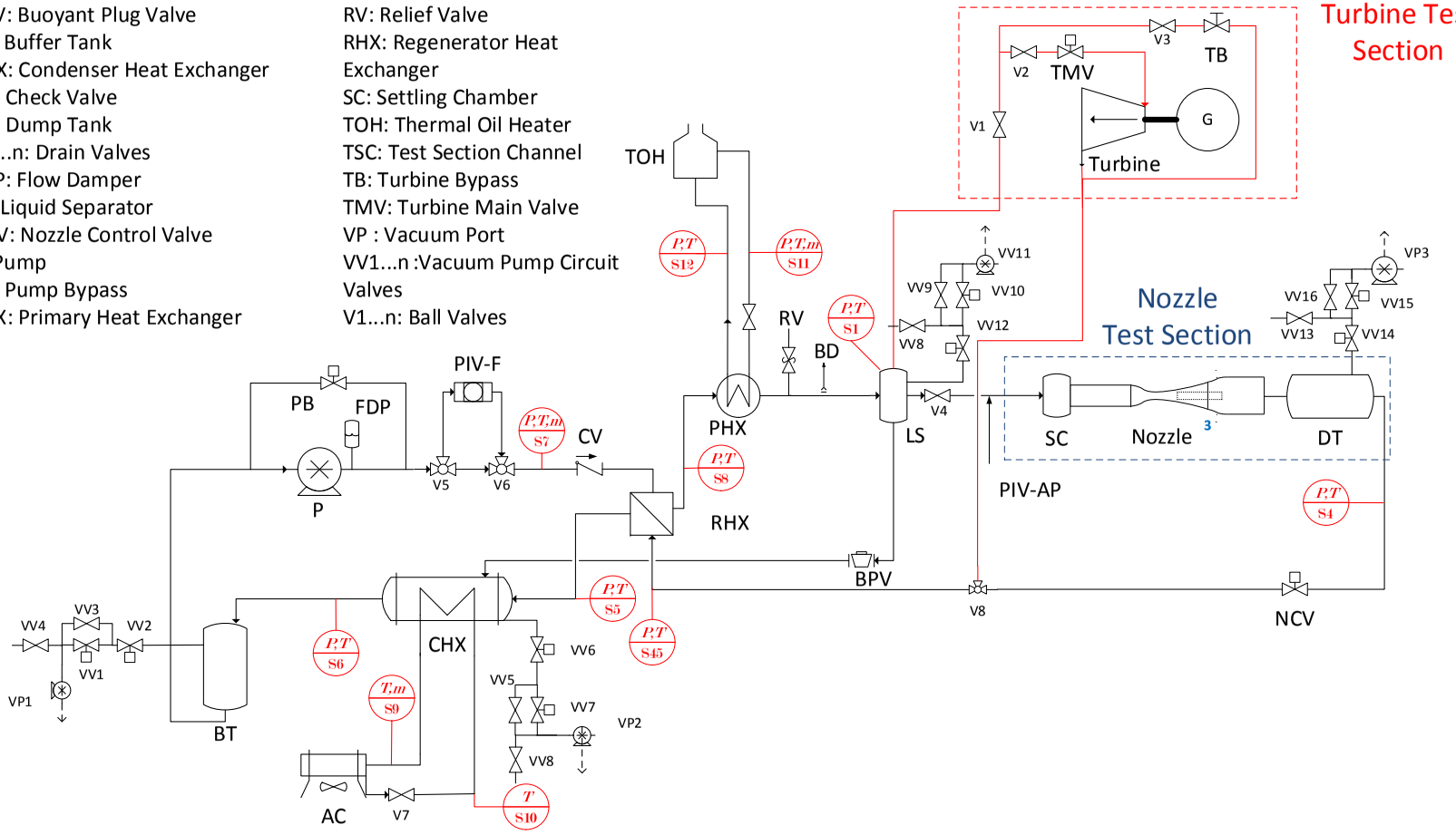

Figure 4.2: Detailed process flow diagram of the ORCHID facility, including the measurement stations (in red).

Bibliography

[1] G. Angelino and C. Invernizzi. Experimental investigation on the thermal stability of some new zero ODP refrigerants. International Journal of Refrigeration, 26(1):51 – 58, 2003.

[2] G. Angelino, C. Invernizzi, and E. Macchi. Organic working fluid optimization for space power cycles. In G. Angelino, L. De Luca, and W.A. Sirignano, editors, Modern Research Topics in Aerospace Propulsion. Springer New York, 1991.

[3] M. Astolfi, M.C. Romano, P. Bombarda, and E. Macchi. Binary ORC (organic Rankine cycles) power plants for the exploitation of medium-low temperature geothermal sources - Part A: Thermodynamic optimization. Energy, 66:423–434, 2014.

[4] M. Astolfi, M.C. Romano, P. Bombarda, and E. Macchi. Binary ORC (organic Rankine cycles) power plants for the exploitation of medium-low temperature geothermal sources - Part B: Techno-economic optimization. Energy, 66:435–446, 2014.

[5] S. Bahamonde, M. Pini, and P. Colonna. Simultaneous turbine and thermodynamic optimization for high-temperature mini-ORC turbogenerators. 2015. Submitted for Publication.

[6] W. H. Pope A. Barlow, J. B. Rae. Low Speed Wind Tunnel Testing. John Wiley and Sons, 1999.

[7] B.P. Brown and B.M. Argrow. Application of Bethe-Zel'dovich-Thompson fluids in organic Rankine cycle engines. Journal of Propulsion and Power, 16(6):1118–1124, 2000.

[8] E. Casati, S. Vitale, M. Pini, G. Persico, and P. Colonna. Centrifugal turbines for Mini-ORC power systems. Journal of Engineering for Gas Turbines and Power-Transactions of the ASME, 136(12):122607–1–11, 2014.

[9] P. Colonna. Fluidi di Lavoro Multi Componenti Per Cicli Termodinamici di Potenza (Multicomponent Working Fluids for Power Cycles). PhD thesis, Politecnico di Milano, 1996.

[10] P. Colonna, E. Casati, C. Trapp, T. Mathijssen, J. Larjola, T. Turunen-Saaresti, and A. Uusitalo. Organic Rankine cycle power systems: From the concept to current technology, applications, and an outlook to the future. Journal of Engineering for Gas Turbines and Power-Transactions of the ASME, 137:100801–1–19, 2015.

[11] P. Colonna and A. Guardone. Molecular interpretation of nonclassical gas dynamics of dense vapors under the van der Waals model. Physics of Fluids, 18(5):056101–1–14, 2006.

[12] P. Colonna, A. Guardone, and N. R. Nannan. Siloxanes: a new class of candidate Bethe-Zeldovich-Thompson fluids. Physics of Fluids, 19(8), 2007.

[13] P. Colonna, J. Harinck, S. Rebay, and A. Guardone. Real-gas effects in organic Rankine cycle turbine nozzles. Journal of Propulsion and Power, 24(2):282–294, 2008.

[14] P. Colonna, N. Nannan, A. Guardone, and E.W. Lemmon. Multiparameter equations of state for selected siloxanes. Fluid Phase Equilibria, 244:193–211, 2006.

[15] P. Colonna, T. P. van der Stelt, and A. Guardone. FluidProp (Version 3.0): A program for the estimation of thermophysical properties of fluids, 2012. A program since 2004.

[16] F2 Chemicals Limited. Flutec pp2 datasheet, 2015. Available online at http://f2chemicals.com/pdf/sds/FLUTEC%20PP2%20-%20SDS20123%20-%20ENG.pdf [Accessed May 2015].

[17] D. M. Ginosar, L. M. Petkovic, and D. P. Guillen. Thermal stability of cyclopentane as an organic Rankine cycle working fluid. Energy Fuels, 25(9):4138–4144, 2011.

[18] A. Guardone, P. Colonna, E. Casati, and E. Rinaldi. Non-classical gas dynamics of vapour mixtures. Journal of Fluid Mechanics, 741:681–701, 2014.

[19] A. Guardone, C. Zamfirescu, and P. Colonna. Maximum intensity of rarefaction shock waves for dense gases. Journal of Fluid Mechanics, 642:127–146, 2010.

[20] J. Harinck, P. Colonna, A. Guardone, and S. Rebay. Influence of thermodynamic models in two-dimensional flow simulations of turboexpanders. Journal of Turbomachinery, 132(1), 2010.

[21] J. Harinck, A. Guardone, and P. Colonna. The influence of molecular complexity on expanding flows of ideal and dense gases. Physics of Fluids, 21(8):086101–1–14, 2009.

[22] K. Hasselmann, F. Reinker, S. Wiesche, E. Y. Kenig, F. Dubberke, and Vrabec J. Performance predictions of axial turbines for organic Rankine cycle (ORC) applications based on measurements of the flow through two-dimensional cascades of blades. In Proceedings of the ASME 2014 Power Conference, 2014.

[23] V.N. Havens, D.R. Ragaller, L. Silbert, and D. Miller. Toluene stability space station rankine power systems. Proceedings of the 22nd Intersociety Energy Conversion Engineering Conference (IECEC), Philadelphia, PA, August 10-14 1987.

[24] A. J. Head, C. De Servi, M. Pini, and P. Colonna. Design of the ORCHID: An experimental facility for ORC nozzle and turbine testing. 2015. Submitted for Publication.

[25] C. Invernizzi. Closed power cycles - thermodynamic fundamentals and applications. In Lecture Notes in Energy, number 11. Springer-Verlag, 2013.

[26] E.W. Lemmon, M.L. Huber, and M.O. McLinden. NIST standard reference database 23: Reference fluid thermodynamic and transport properties-REFPROP, version 9.0. National Institute of Standards and Technology, Standard Reference Data Program, Gaithersburg, 2010.

[27] N. P. Leslie, O. Zimron, R. S. Sweetser, and T. K. Stovall. Recovered energy generation using an organic Rankine cycle system. ASHRAE Transactions, 115 (Part I):220–230, 2009.

[28] E. Macchi. Design criteria for turbines operating with fluids having a low speed of sound. Lecture Series 100, Von Karman Institute for Fluid-dynamics, Bruxelles, 1977.

[29] M. J. Moran and H. N. Shapiro. Fundamentals of Engineering Thermodynamics. John Wiley & Sons, 3rd edition, 1998.

[30] N. R. Nannan, A. Guardone, and P. Colonna. On the fundamental derivative of gas dynamics in the vapor-liquid critical region of single-component typical fluids. Fluid Phase Equilib., 337:259–273, January 2013.

[31] M. Pasetti, C.M. Invernizzi, and P. Iora. Thermal stability of working fluids for organic Rankine cycles: An improved survey method and experimental results for cyclopentane, isopentane and n-butane. Applied Thermal Engineering, 73(1):762–772, 2014.

[32] M. Pini, G. Persico, E. Casati, and V. Dossena. Preliminary design of a centrifugal turbine for organic Rankine cycle applications. Journal of Engineering for Gas Turbines and Power-Transactions of the ASME, 135:042312–1–9, 2013.

[33] A. Pope. Wind tunnel calibration techniques. Technical report, NATO, 1961.

[34] A. Pope and K.L. Goin. High-Speed Wind Tunnel Testing. John Wiley and Sons, 1965.

[35] A. Spinelli, M. Pini, V. Dossena, P. Gaetani, and F. Casella. Design, simulation, and construction of a test rig for organic vapors. J. Eng. Gas Turbines Power, 135(4):10, March 2013.

[36] P.A. Thompson. A fundamental derivative in gasdynamics. Physics of Fluids, 14(9):1843–1849, 1971.

[37] J.P. van Buijtenen. The Tri-O-Gen organic Rankine cycle: Development and perspectives. Journal of the IDGTE Power Engineering, 13:4–12, August 10-14 2009.

[38] T. Weith, F. Heberle, Preissinger M., and Bruggemann D. Performance of siloxane mixtures in a high-temperature organic Rankine cycle considering the heat transfer charactersitics during evaporation. Energies, 7:5548– 5565, 2014.

[39] C. Zamfirescu, A. Guardone, and P. Colonna. Admissibility region for rarefaction shock waves in dense gases. Journal of Fluid Mechanics, 599:363–381, 2008.

[40] G. J. Zyhowski. Honeywell Refrigerants Improving the Uptake of Heat Recovery Technologies. Available online at http://www.honeywell-orc.com/wp-content/uploads/2011/09/Honeywell-Refrigerants-Improve-Uptake-Heat-Recovery-Technologies.pdf [Accessed May 2015].